R. & M. No. 2529
(9,360)
(A.R.C. Technical Report)

MINISTRY OF SUPPLY

AERONAUTICAL RESEARCH COUNCIL
REPORTS AND MEMORANDA

The Theoretical Effect of Flight Path Angle on the Lateral Stability and Response of an Aircraft

By

E. M. FRAYN, B.Sc., and M. V. PARNELL

LONDON: HER MAJESTY'S STATIONERY OFFICE
1954
PRICE 7s 6d NET

The Theoretical Effect of Flight Path Angle on the Lateral Stability and Response of an Aircraft

By

E. M. FRAYN, B.Sc., and M. V. PARNELL

COMMUNICATED BY THE PRINCIPAL DIRECTOR OF SCIENTIFIC RESEARCH (AIR), MINISTRY OF SUPPLY

Reports and Memoranda No. 2529*

November, 1945

Summary.—The response of a typical aircraft of the dive-bomber class to various disturbances has been calculated at four angles of dive covering the range 0 to 90 deg and for four pairs of values of l_v, n_v. The most notable effect on stability is the marked increase in spiral damping with increasing dive angle at the same T.A.S. This has little effect on the response, since in most components, this mode is scarcely excited.

For dive angles up to 30 deg the variations in response are so slight as to be negligible, while for larger angles of dive the variation is small for the first 2 airsecs. Calculations of response in level flight, which slightly underestimate the response in a dive, can thus be assumed to give a sufficiently accurate picture of the behaviour at small flight path angles for most requirements.

1. *Introduction.*—Many surveys of the stability and response of aircraft in level flight have been made but little work has been done at other flight-path angles. Information was required regarding the behaviour of an aircraft in a dive at high speed and the importance of dive angle as a variable. In this report the stability and response at various angles of dive at the same T.A.S. have been examined with the object of solving these problems.

It is assumed that the small variations of elevator and thrust necessary to maintain the initial attitude and T.A.S. are made. Density changes are ignored since they will have no effect at this low Mach number ($M = 0{\cdot}41$); in adding dimensional units it is further assumed that the dive is done at ground level as a near approach to a dive-bombing attack. It was considered that little accuracy was lost by these assumptions, which greatly ease computation.

The equations of motion are used in the linear form, which is valid for small displacements. They are solved by operational methods using the Laplace transformation[1] and modal response coefficients[2], and from them response curves are calculated. The problem has been studied mainly by the use of response coefficients, since they show more clearly than do the response curves the changes produced by varying any one parameter. Some response curves are given to illustrate the argument.

It should be noticed that in the equations of motion the angles of bank and yaw, ϕ and ψ, are not used with the standard definitions of R. & M. 1801[3]. A full discussion of both the old and new definitions is given in section 2 and is illustrated by Fig. 1.

2. *Equations of Motion and their Solution.*—2.1. *Definition of the Angles* ψ, θ, ϕ.—The equations of R. & M. 1801[3] are unsuitable for use in work in which a steep angle of dive is considered chiefly because they fail where $\gamma_e = -90$ deg and further because they refer the angles ϕ and ψ to a

* R.A.E. Report Aero. 2097, received 4th February, 1946.

hypothetical position of the aircraft in a horizontal plane. To avoid these difficulties the angles ϕ and ψ are now measured from the plane defined by the wings and the direction of motion; ϕ is then a rotation about the direction of motion and ψ a rotation in this plane about the line through the centre of gravity perpendicular to the plane. An initial displacement ϕ_e is considered for the sake of completeness, although this involves the consideration of unsymmetrical flight.

The new definitions are illustrated by Fig. 1a. The configuration in steady motion is reached by two rotations; first the axis $G\bar{x}$ is inclined upwards at an angle γ_e to the horizontal and then $G\bar{y}$ and $G\bar{z}$ are rotated about $G\bar{x}$ from $G\bar{y}$ towards $G\bar{z}$ through an angle ϕ_e from the position in which $G\bar{y}$ is horizontal. This brings the aircraft to the position $G\bar{x}\bar{y}\bar{z}$. The configuration in disturbed motion, $Gxyz$, is reached by three consecutive rotations. The first is about $G\bar{z}$, from $G\bar{x}$ towards $G\bar{y}$, through an angle ψ bringing these axes to the intermediate positions Gx_1, Gy_1; next comes a rotation about Gy_1, from $G\bar{z}$ towards Gx_1 through an angle θ bringing $G\bar{z}$ to the intermediate position Gz_1 and Gx_1 to its final position Gx; lastly there is a rotation about Gx from Gy_1 towards Gz_1 through an angle ϕ bringing these axes to their final positions Gy and Gz.

The way in which the definitions of R. & M. 1801 differ from these can be seen in Fig. 1b. Here initial ϕ_e is not considered, since this is equivalent to a change in the origin of ϕ. The first rotation in this system is about $G\bar{z}$ from $G\bar{x}$ towards $G\bar{y}$ through an angle ψ, bringing these axes to the intermediate positions Gx_1, Gy_1. Next we consider a rotation about Gy_1, from $G\bar{z}$ towards Gx_1 through an angle γ_e, which brings these axes to the positions Gz_1 and Gx_2; the next rotation is about the same axis and in the same direction and brings Gz_1 to the further intermediate position Gz_2 and Gx_2 to its final position Gx. The final rotation about the axis Gx from Gy_1 towards Gz_2 brings Gy_1 and Gz_2 to their final positions Gy and Gz.

If, the ϕ and ψ of R. & M. 1801 are termed ϕ' and ψ' they are expressed in terms of the newly defined ϕ and ψ by the relations

$$\left.\begin{aligned} \psi' &= \psi \sec \gamma_e \\ \phi' &= \phi + \psi \tan \gamma_e \end{aligned}\right\} \quad \ldots \quad (2.1.1)$$

The failure of the R. & M. 1801 definitions when $\gamma_e = 90$ deg is obvious from the formulae (2.1.1). When $\gamma_e = 90$ deg both $\sec \gamma_e$ and $\tan \gamma_e$ are infinite so that the old definitions of ϕ and ψ become meaningless.

Also when dive bombing at a fairly steep angle the pilot will wish to correct his line error in the plane in which he is diving. For this the error in yaw, ψ, in the plane in which the aircraft is flying is required, not the angle ψ' which is $\sec \gamma_e$ times as large. This latter angle would give a quite erroneous idea of the manoeuvrability of the aircraft.

In mathematical work on response we generally consider the effect of control application or of a side gust. If, however, a complete manoeuvre is being considered a necessary final condition, if there is to be no sideslip, is that the angle of the wings to the horizontal should be zero. The main disadvantage of this new system of angles is that ϕ is not the angle of the wings to the horizontal; the angle ϕ' can, however easily be calculated from the formulae (2.1.1). Provided the aircraft has only a small angle of yaw and is not diving steeply the correction term will be small.

The new definitions have the further merit of simplifying two of the equations of motion* which become

$$\left.\begin{aligned} \hat{p} &= \frac{d\phi}{d\tau} \\ \hat{r} &= \frac{d\psi}{d\tau} \end{aligned}\right\} \quad \ldots \quad (2.1.2)$$

* The equations in this form have been used by the Instrument Department in work on Automatic Controls.

2.2. *Equations of Motion.*—The equations of motion were considered in the form valid for small disturbances, which with the new definitions of ϕ and ψ become:

$$\left.\begin{array}{lllll}
\left\{\dfrac{d}{d\tau}+\bar{y}_v\right\}\hat{v} & & +\hat{r}-k\phi+k'\psi & & =0 \\
\mathscr{L}\hat{v}+\left\{\dfrac{d}{d\tau}+l_1\right\}\hat{p} & & -l_2\hat{r} & & =\mathscr{C}_l \\
-\mathscr{N}\hat{v}+ & n_1\hat{p}+\left\{\dfrac{d}{d\tau}+n_2\right\}\hat{r} & & & =\mathscr{C}_n \\
 & -\hat{p} & +\dfrac{d\phi}{d\tau} & & =0 \\
 & & -\hat{r} & +\dfrac{d\psi}{d\tau} & =0
\end{array}\right\}, \quad \ldots \ldots \quad (2.2.1)$$

where τ is the time in airsecs. The unit of aerodynamic time $\hat{t}$ is given by the equation

$$\hat{t} = W/g\rho SU_e \quad \text{true secs,} \quad \ldots \ldots \ldots \ldots \ldots \quad (2.2.2)$$

where W is the weight of the aircraft (lb), ρ the air density (slugs/ft^3), g the acceleration due to gravity (ft/sec^2), U_e the forward velocity of the aircraft (ft/sec), S is the wing area (ft^2), and γ_e is the angle of climb, and the modified derivatives are

$$\left.\begin{array}{llll}
l_1=-\dfrac{l_p}{i_{A'}} & , & n_1=-\dfrac{n_p}{i_{C'}} & , \\
l_2=\dfrac{l_r}{i_{A'}} & , & n_2=-\dfrac{n_r}{i_{C'}} & , \\
\mathscr{L}=-\dfrac{\mu_2 l_v}{i_{A'}} & , & \mathscr{N}=\dfrac{\mu_2 n_v}{i_{C'}} & , \\
\mathscr{C}_l=\dfrac{\mu_2 C_l}{i_{A'}} & , & \mathscr{C}_n=\dfrac{\mu_2 C_n}{i_{C'}} & , \\
\bar{y}_v=-y_v & , & k'=-k\tan\gamma_e\,, &
\end{array}\right\} \quad \ldots \ldots \ldots \quad (2.2.3)$$

the quantities l_p, l_r, n_p, n_r, l_v, n_v, y_v, k, μ_2, C_l, C_n, $i_{A'}$, $i_{C'}$, having the definitions of Ref. 3. Further, $\hat{p}$ and $\hat{r}$ are the angular velocities of bank and yaw in radn/airsec, and $\hat{v}$, ϕ, ψ are the angles of sideslip, bank and yaw in radians.

2.3. *Solution of the Equations and the Cases Considered.*—The equations were solved by the methods of the Laplace transformation[1] for various applied forces and moments. The conditions considered were a constant applied rolling moment, a constant applied yawing moment, and initial angles of sideslip, bank and yaw. Modal response coefficients[2] were evaluated for all these applied forces and from these response curves were calculated.

The stability parameters were chosen to be typical of a medium-size dive bomber of span $b = 60$ ft, wing loading 46 lb/ft^2 moving with velocity $U_e = 454$ ft/sec or 270 knots T.A.S. at sea level. The velocity was assumed to be independent of dive angle; l_r and n_p were varied with C_L each being proportional to $\cos\gamma_e$. The values taken are given by the following table:

$-\gamma_e$ deg	C_L	l_r	n_p	k
0	0·1875	0·06	−0·03	0·09375
30	0·1624	0·052	−0·026	0·0812
60	0·094	0·03	−0·015	0·047
90	0	0	0	0

.. (2.3.1)

Further

$$\left.\begin{aligned} l_p &= -0\cdot42 \\ \bar{y}_v &= 0\cdot2 \\ i_{A'} &= 0\cdot12 \\ i_{C'} &= 0\cdot18 \\ \varepsilon_A = \varepsilon_C &= 0 \\ \mu_2 &= 20 \end{aligned}\right\} , \qquad \ldots \qquad (2.3.2)$$

and

$$\left.\begin{aligned} n_r &= n_{r0} - n_v \\ n_{r0} &= -0\cdot024 \end{aligned}\right\} \qquad \ldots \qquad (2.3.3)$$

where

Calculations were made for four pairs of values of l_v, n_v formed by taking all possible combinations of the values

$$\left.\begin{aligned} l_v &= 0 \quad , \quad -0\cdot12 \\ n_v &= 0\cdot024 \quad , \quad 0\cdot096 \end{aligned}\right\} \qquad \ldots \qquad (2.3.4)$$

Thus the l_v, n_v combinations considered are sufficiently wide to indicate the effect of dive angle for any values of these parameters.

For the typical aircraft of span 60 ft, wing loading 46 lb/ft², the unit of aerodynamic time is 1·32 seconds at sea level for all conditions considered. The lateral relative density μ_2 is

$$\mu_2 = \frac{2W}{g\rho Sb} , \qquad \ldots \qquad (2.3.5)$$

where b is the span (ft), so it is possible to regard these results as applying for example to an aircraft of span 70 ft, with a wing loading of 53·6 lb/ft² diving at the same speed but with $\hat{t} = 1\cdot54$ sec.

The values of $-\gamma_e$ used in the calculations,

$$-\gamma_e = 0, 30, 60, 90 \text{ deg} \qquad \ldots \qquad (2.3.6)$$

were considered to cover the range $-\gamma_e = 0$ to 90 deg adequately.

3. *Effect of Angle of Dive on Stability*.—The roots of a stability biquadratic

$$\lambda^4 + B\lambda^3 + C\lambda^2 + D\lambda + E = 0 \qquad \ldots \qquad (3.1)$$

were evaluated for each pair of values of l_v, n_v at the four flight path angles and are given in Table 1.

When $-\gamma_e = 90$ deg the biquadratic (3.1) becomes

$$(\lambda + l_1)\{\lambda^3 + (n_2 + \bar{y}_v)p^2 + (n_2\bar{y}_v + \mathcal{N})p + \mathcal{N}k'\} = 0\,. \qquad \ldots \qquad \ldots \qquad (3.2)$$

The derivatives l_r and n_p are zero in vertical flight, hence there is no term in $\hat{p}$ except in the rolling equation. Thus the rolling motion separates out, the roots are independent of l_v and the rolling root is exactly equal to $-l_1$. Approximate values of the other roots are given by the formulae

$$\left.\begin{aligned} \lambda_1 &= -k' && \text{(spiral mode)} \\ r &= \tfrac{1}{2}(n_2 + \bar{y}_v - k') && \text{(oscillation damping)} \\ s^2 &= \mathcal{N} + n_2(\bar{y}_v - k') && \text{(frequency}^2\text{)} \end{aligned}\right\} \qquad \ldots \qquad \ldots \qquad (3.3)$$

Thus variations in n_2 and $\bar{y}_v$ will have a fairly large effect only on the oscillation damping, and these changes will not be serious unless the change in n_2 or $\bar{y}_v$ is large. Since it has also been shown[4,5] that variations in the rotary derivatives have little effect on the early stages of response in level flight it is permissible to regard these results as applying to different aircraft with approximately the same coefficients of inertia, and not only to the typical one whose derivatives have been used in the calculations.

The effect of angle of dive on the damping of the oscillation is best studied by considering the number of swings to halve amplitude, which are listed in Table 2. Here there is an improvement with increase of $-\gamma_e$ when $l_v = -0 \cdot 12$, particularly when n_v is small, but with zero l_v there is a slight increase in the number of swings to halve amplitude as $-\gamma_e$ increases. This is due to the damping r which increases or decreases with $-\gamma_e$ according as l_v is large or small. An examination of the approximate formulae for level and vertical flight shows that this will occur in general. It may be noted that the period of the oscillation is almost independent of the angle of dive and l_v, but varies considerably with n_v, being greatly lengthened when n_v is small.

Table 1 shows that the absolute damping of the oscillation is never large; its greatest value of $0 \cdot 443$ when $l_v = 0$, $n_v = 0 \cdot 096$, $\gamma_e = 0$, gives a time to half-amplitude of $2 \cdot 07$ sec. This might be thought tolerably good until it is compared with the period of $2 \cdot 54$ sec, when it is seen that several complete swings are necessary to damp the oscillation down to a negligible magnitude. Since the oscillation even in this case is likely to be troublesome it is to be hoped that it is not greatly excited in the motion.

The spiral damping increases with an increasing angle of dive and is practically insensitive to changes in l_v, n_v at large values of $-\gamma_e$. Spiral instability is encountered only in level flight with zero l_v, but as the time to double amplitude is about 70 true seconds the instability is not serious.

In general the stability of an aircraft in a dive is better than its stability in level flight, the slight shortening of the period of the oscillation being compensated for by the increase of damping except when both l_v and n_v are small. In all cases there is a definite increase in spiral stability with increase of $-\gamma_e$ and progressive changes in the roots occur as $-\gamma_e$ increases from 0 to 90 deg.

Most of the change in the roots between $\gamma_e = 0$ and -90 deg occurs between $\gamma_e = 0$ and -60 deg. This differs greatly from the manner of change of the response in which it will be shown that the greatest variation is between $-\gamma_e = 60$ and 90 deg.

4. *Response*.—4.1. *Interpretation of Modal Response Coefficients*.—The variations with dive angle of the response to various disturbances can most easily be studied by a consideration of the modal response coefficients and the corresponding roots of the stability equations, which are listed in Tables 3 to 7. The response to an initial displacement or impulsive force is given by an expression of the form

$$\frac{\hat{v}}{\phi_0} = v_1\alpha_{1\phi}e^{\lambda_1\tau} + v_2\alpha_{2\phi}e^{\lambda_2\tau} + 2|v_3\alpha_{3\phi}|e^{-r\tau}\sin(s\tau + \beta_\phi + \gamma_v) + Q_{v\phi}\,, \qquad \ldots \qquad \ldots \qquad (4.1)$$

where $\hat{v}/\phi_0$ is the value of $\hat{v}$ due to an initial angle of bank $\phi_0 = 1$, $Q_{v\phi}$ is a constant determined by the initial conditions (in this case $\hat{v} = 0$ when $\tau = 0$), β_ϕ is the part of the phase angle dependent on the disturbance and γ_e the part dependent on the component. Similarly response to a finite applied moment is given by an expression of the form

$$\frac{\hat{v}}{\mathscr{C}_l} = v_1\alpha_{1l}\frac{1 - e^{\lambda_1\tau}}{-\lambda_1} + v_2\alpha_{2l}\frac{1 - e^{\lambda_2\tau}}{-\lambda_2} + \frac{2|v_3\alpha_{3l}|}{(r^2 + s^2)^{1/2}} e^{-r\tau} \sin(s\tau + \beta_l + \gamma_v) + R_{vl}\tau + K_{vl} ,$$

where $\hat{v}/\mathscr{C}_l$ is the value of $\hat{v}$ due to an applied rolling moment $\mathscr{C}_l = 1$, and R_{vl} and K_{vl} are determined from the initial conditions (in this case $\hat{v} = 0$ when $\tau = 0$), R_{vl} having non-zero values only in ϕ and ψ, and β_l and γ_v being the components of the phase angle as defined above.

The relative amplitudes associated with the components $\hat{v}$, $\hat{p}$, etc., in the spiral mode are denoted by v_1, p_1, etc., while α_{1v}, $\alpha_{1\phi}$, etc., define the magnitudes of excitation of the mode by initial displacements $\hat{v}_0 = 1$, $\phi_0 = 1$, etc. Thus the product $v_1\alpha_{1\phi}$ is the amplitude of $\hat{v}$ due to the excitation of the spiral mode by an initial rate of roll $\phi_0 = 1$. The same quantities with suffix 2 refer to the rolling subsidence. The amplitude in $\hat{v}$ due to the excitation of the oscillation by an initial angle of bank is $2|v_3\alpha_{3\phi}|$, $(\beta_l + \gamma_v)$, etc., being the phase angle as defined above.

In Tables 3, 6, and 7 (response to a side gust and to initial angles of bank and yaw) are listed $v_1\alpha_{1v}$, $v_2\alpha_{2v}$, $2|v_3\alpha_{3v}|$, Q_{vv} and the corresponding quantities for other components, together with the roots of the stability biquadratic. In Tables 4 and 5 are listed $v_1\alpha_{1l}/\lambda_1$, $v_2\alpha_{2l}/\lambda_2$, $2|v_3\alpha_{3l}|/(r^2 + s^2)^{1/2}$, etc., and in Table 8 are the phase angles for all disturbances.

The rolling subsidence (λ_2) is heavily damped and has an appreciable effect on the motion only in its early stages. Its importance decreases with increasing angle of dive and is greatest in $\hat{p}$ and ϕ.

The spiral mode (λ_1) is a divergence with small $-l_v$ in level flight and acquires increasing stability with increase in $-l_v$ and angle of dive. It is a combined rolling and yawing motion in which the rolling component disappears in the vertical dive when $l_v = 0$.

The lateral oscillation is excited to anamplitude $2|v_3\alpha_{3v}|$, etc., by an initial displacement or impulsive force and $2|v_3\alpha_{3l}|/(r^2 + s^2)^{1/2}$, etc., by a finite applied moment. It affects the angle of sideslip at all l_v, n_v having the greatest influence on the yawing motion at large n_v and on the rolling motion at large $-l_v$. In the vertical dive at $l_v = 0$ its contribution to the rolling motion is zero. The difference between the phase angles (γ_v, etc.) for different components is the same for all disturbances. The angle of dive has very little effect on phase angle.

Fig. 2 shows the contributions of the three modes to the response in rate of roll to applied rolling moment. The contribution due to the spiral root is $p_1\alpha_{1l}\dfrac{1 - e^{\lambda_1\tau}}{-\lambda_1}$, that due to the rolling root is $p_2\alpha_{2l}\dfrac{1 - e^{\lambda_2\tau}}{-\lambda_2}$ and the oscillatory term combined with the phase angle is

$$\frac{2|p_3\alpha_{3l}|}{r^2 + s^2} e^{-r\tau} \cos(s\tau + \beta_l + \gamma_p).$$

The coefficient of the linear term is zero. The total response curve obtained by adding these three terms is shown by the dotted line. The response to an initial angle of bank can be split up into its three components in the same way but in this case the response coefficients $p_1\alpha_{1\phi}$, $p_2\alpha_{\phi 2}$ would multiply $e^{\lambda_1\tau}$, $e^{\lambda_2\tau}$ while the coefficient of $e^{-r\tau}\cos(s\tau + \beta_\phi + \lambda_p)$ would be $2|p_3\alpha_{3\phi}|$. When this interpretation of the modal response coefficients is understood changes in response due to variations of flight path angle can be easily seen from these tables.

4.2. *Response to a Side Gust.*—Table 3 shows that in response to a side gust the excitation of the spiral mode is small and is appreciable only in ϕ and ψ, the magnitude of excitation being insensitive to changes in l_v, n_v. Fig. 3 showing $\phi/\hat{v}_0$ for $n_v = 0{\cdot}024$, $l_v = -0{\cdot}12$, illustrates the small effect of changes in this root, which varies from $-0{\cdot}0256$ at $\gamma_e = 0$ deg to $-0{\cdot}0931$ at $-\gamma_e = 90$ deg, for the values of the parameters taken: variations in the spiral root are made apparent by changes in the centre of oscillation which becomes more negative as $-\gamma_e$ increases. The variations in the period, damping, and excitation of the oscillation are more noticeable: as $-\gamma_e$ increases the period and damping are increased. The increased effect of the rolling root can be seen from the increase in the initial peak as $-\gamma_e$ increases: variations associated with this root are, however, small.

The increased period and damping of the oscillation are again shown by the rate of yaw for $l_v = -0\cdot 12$, $n_v = 0\cdot 024$ (Fig. 4) when the initial amplitude $2|v_3\alpha_{3v}|$ does not vary appreciably with γ_e. The spiral mode has little effect on the motion while the decrease in the first peak with increasing angle of dive is due to the decrease of the yawing component of the rolling subsidence.

When $l_v = 0$ the excitation of the rolling subsidence decreases with increasing angle of dive as do those of the spiral and oscillatory modes in $\hat{p}$ and ϕ. Fig. 5, showing angles of bank for $l_v = 0$, $n_v = 0\cdot 024$, shows the relatively large changes caused by these variations.

In general, although the change in response from $\gamma_e = 0$ to -90 deg is considerable, the curves for $-\gamma_e = 0$ and 30 deg never differ by more than 30 per cent in the first 3 airsec (4 true sec). Thus, as was indicated by the response coefficients, the variations of the spiral root have little effect on the motion.

4.3. *Response to Applied Rolling Moment.*—When $-\gamma_e = 90$ deg the response to applied rolling moment is, as was to be expected from the equations of section 3, that of simple rolling theory. Thus $\hat{p}$ is the exponential $(1 - e^{-l_1\tau})$ and $\hat{v}$, $\hat{r}$ and ψ are all zero. The vertical dive is the limiting case towards which the response will tend with increasing $-\gamma_e$, hence it is natural that aileron response should improve as the steepness of the dive increases, but it is notable that there is a great difference between the response at 60 deg and 90 deg.

The coefficients of response to an applied rolling moment are given in Table 4. The excitation of the spiral mode decreases with increasing angle of dive while that of the rolling subsidence remains approximately constant; the excitation of the oscillation is greatest for large l_v and small n_v but it decreases with increasing dive angle to become zero at $\gamma_e = -90$ deg. Figs. 6 and 7 show that the total effect of variations in γ_e on response is small when $l_v = 0$.

Figs. 8 to 12 show response in $\hat{p}$, $\hat{v}$, $\hat{r}$, ϕ and ψ to applied rolling moment for two pairs of values of l_v, n_v and illustrate these points. It is interesting to note that although the magnitude of the adverse yawing motion decreases as $-\gamma_e$ increases its duration remains constant.

4.4. *Response to Applied Yawing Moment.*—The coefficients for response to applied yawing moment which are given in Table 5 show similar variations in the coefficients associated with the spiral root; the contribution of the rolling root is approximately independent of γ_e. The initial amplitude of the oscillation does not vary much from $-\gamma_e = 0$ to 30 deg, but there is a fairly large change as $-\gamma_e$ increases beyond that value notably in $\hat{p}$ and ϕ when $l_v = -0\cdot 12$. This is illustrated in Fig. 13, which shows response in rate of roll to an applied yawing moment. The greatest change in response is again between $\gamma_e = -60$ and -90 deg.

4.5. *Response to Initial Angles of Bank and Yaw.*—Tables 6 and 7 contain the response coefficients for initial angles of bank and yaw. Here again the large variations in the excitation of the spiral mode are not reflected in the curves owing to accompanying variations of the constant term. The comparatively small changes of angle of yaw with γ_e for $n_v = 0\cdot 024$, $l_v = -0\cdot 12$ are illustrated by Fig. 14, which shows the response in ψ to initial angle of bank. Here, too, it is clear that variations in the spiral root do not greatly affect the motion.

5. *Discussion and Conclusions.*—The table of response coefficients shows that, in general, change of flight path angle does not seriously affect response. The full set of curves show that variations are least when both l_v and n_v are large and are such that the response is improved as the angle of dive increases. It is clear from both the coefficients and the curves that the change in response when $-\gamma_e$ varies from 0 to 30 deg is so small that it can reasonably be disregarded in calculations.

The variation in response is less than was suggested by an examination of the stability roots; this is due to the fact that at this low value of the lift coefficient the spiral mode, which is the mode most affected by variation of γ_e, is not greatly excited. It is interesting to see this lack of correlation between stability and response, which was also noted in R. & M. 2294[4,5]. It is probable that at higher values of C_L, *i.e.*, at lower speed, the variation of response with γ_e will be greater though still small in the range $-\gamma_e = 0$ to 30 deg.

It can thus be concluded that if the stability and response of an aircraft are satisfactory in level flight they will be slightly better in a dive. Further if a shallow dive ($-\gamma_e < 30$ deg) is being considered it is possible to predict the behaviour of the aircraft with reasonable accuracy from knowledge of its response when $\gamma_e = 0$ deg. This eliminates the need for special calculations when qualitative estimates of the response in a dive of a dive bomber are required, provided that its behaviour in level flight is known. It has further been shown that the response changes progressively with increasing dive angle from that of level flight to that of the simple limiting case of vertical flight; this change is most rapid at the 60–90 deg end of the range.

LIST OF SYMBOLS

A'	Rolling moment of inertia
b	Span, section 2.1
B	Coefficient of cubic term in stability equation, section 3
C	Coefficient of square term in stability equation, section 3
C'	Yawing moment of inertia
C_L	Lift coefficient, section 2.3
C_l, C_n	Coefficients of rolling moment and yawing moment, section 2.2
$\mathscr{C}_l$, $\mathscr{C}_n$	Modified coefficients of rolling moment and yawing moment, section 2.2
D	Coefficient of linear term in stability equation, section 3
E	Constant term in stability equation, section 3. Product of inertia with respect to xz-axes
g	Acceleration due to gravity, section 2.2
i_A'	Rolling inertia coefficient, section 2.2
i_C'	Yawing inertia coefficient, section 2.2
k	$\frac{1}{2}C_L$, section 2.2
k'	$-k \tan \gamma_e$, section 2.2
K_{vl}, etc.	A constant, section 4
$\mathscr{L}$	$-\mu_2 l_v / i_{A'}$, section 2.2
l_1	$-l_p / i_{A'}$, section 2.2
l_2	$l_r / i_{A'}$, section 2.2
l_p, l_r, l_v	Rolling moments due to roll, yaw and sideslip, section 2.2
$\mathscr{N}$	$\mu_2 n_v / i_{C'}$, section 2.2
n_1	$-n_p / i_{C'}$, section 2.2
n_2	$-n_r / i_{C'}$, section 2.2

n_p, n_r, n_v	Yawing moments due to roll, yaw and sideslip, section 2.2
n_{r0}	Body contribution to n_r, section 2.3
$\hat{p}$	Rolling angular velocity in radn/airsec, section 2.2
$Q_{v\phi}$, etc.	Constant term, section 4
r	Damping of complex roots, section 4
$\hat{r}$	Rate of yaw in radn/airsec, section 2.2
R_{vl}, etc.	Coefficient of linear term, section 4.
s	Coefficient of imaginary part of complex roots, section 4.
S	Wing area, section 2.2
$\hat{t}$	Unit of aerodynamic time (airsec), section 2.2
U_e	Forward velocity of aircraft, section 2.2
$\hat{v}$	Angle of sideslip in radians, section 2.2
v_i	Modal amplitude in sideslip, section 4
W	Weight in lb, section 2.2
y_v	Sideforce due to sideslip, section 2.2
$\bar{y}_v$	$-y_v$, section 2.2
α_{1v}	Modal response coefficient to initial sideslip, section 4.
β_l, etc.	Part of phase angle associated with disturbance, section 4
γ_e	Angle of climb in steady motion, section 2.2
γ_v, etc.	Part of phase angle associated with component, section 4
ε_A	$-E/A'$, section 2.3
ε_C	$-E/C'$, section 2.3
θ	Angle of pitch, section 2.2
λ_i	Roots of stability equation, section 4
μ_2	Lateral relative density, section 2.2
ρ	Air density, section 2.3
τ	Time in airsec, section 2.2
ϕ	Angle of bank, section 2.2
ϕ'	Conventional ϕ, section 2.1
ψ	Angle of yaw or azimuth, section 2.2
ψ'	Conventional ψ, section 2.1

REFERENCES

No.	*Author*	*Title, etc.*
1	H. S. Carslaw and J. C. Jaegar	*Operational Methods in Applied Mathematics.* Clarendon Press, Oxford. 1941.
2	K. Mitchell..	Lateral Response Theory. R. & M. 2297. March, 1944.
3	L. W. Bryant and S. B. Gates	Nomenclature for Stability Coefficients. R. & M. 1801. October, 1937.
4	K. Mitchell, A. W. Thorpe and E. M. Frayn.	The Theoretical Response of a High Speed Aeroplane to a Sidegust. R. & M. 2294. May, 1945.
5	K. Mitchell, A. W. Thorpe and E. M. Frayn.	The Theoretical Response of a High Speed Aeroplane to Applied Rolling and Yawing Moments. R. & M. 2294. May, 1945.

TABLE 1

Stability Roots

$\lambda^4 + B\lambda^3 + C\lambda^2 + D\lambda + E = 0$ has roots $\lambda_1, \lambda_2, -r \pm is$

n_v	l_v	$-\gamma_e$ deg	λ_1	λ_2	r	s
0·024	0	0	0·0130	—3·4820	0·2488	1·6413
		30	—0·0361	—3·4865	0·2220	1·6360
		60	—0·0773	—3·4955	0·1969	1·6303
		90	—0·0931	—3·5	0·1868	1·6280
0·024	—0·12	0	—0·0256	—3·8110	0·0650	1·9585
		30	—0·0656	—3·7744	0·0633	1·9178
		60	—0·0931	—3·6691	0·1022	1·8036
		90	—0·0931	—3·5	0·1868	1·6280
0·096	0	0	0·0132	—3·4934	0·4432	3·2682
		30	—0·0363	—3·4950	0·4177	3·2626
		60	—0·0774	—3·4983	0·3954	3·2556
		90	—0·0932	—3·5	0·3867	3·2524
0·096	—0·12	0	—0·0175	—3·7201	0·3145	3·3766
		30	—0·0617	—3·6927	0·3061	3·3579
		60	—0·0918	—3·6151	0·3299	3·3118
		90	—0·0932	—3·5	0·3867	3·2524

TABLE 2

Periods, Times to Halve Amplitude and Number of Oscillations to Halve Amplitude

n_v	l_v	$-\gamma_e$ deg	Time to $\frac{1}{2}$ ampl. spiral (true sec)	Time to $\frac{1}{2}$ ampl. oscillation (true sec)	Period of oscillation (true sec)	Number of oscillations to $\frac{1}{2}$ ampl.
0·024	0	0	—70·4050	3·6860	5·0657	0·7276
		30	25·3775	4·1310	5·0821	0·8129
		60	11·8691	4·6570	5·0997	0·9132
		90	9·8515	4·9105	5·1070	0·9615
0·024	—0·12	0	35·7924	14·1021	4·2451	3·3220
		30	14·0089	14·4859	4·3352	3·3415
		60	9·8519	8·9763	4·6097	1·9467
		90	9·9515	4·9105	5·1070	0·0615
0·096	0	0	—69·7078	2·0695	2·5439	0·8135
		30	25·2447	2·1960	2·5483	0·8618
		60	11·8438	2·3194	2·5538	0·9082
		90	9·8396	2·3717	2·5563	0·9278
0·096	—0·12	0	52·3196	2·9162	2·4622	1·1844
		30	14·8571	2·9962	2·4760	1·2102
		60	9·9909	2·7804	2·5105	1·1076
		90	9·8396	2·3717	2·5563	0·9278

TABLE 3

Modal Response Coefficients for Response to a Side-gust

(i) *Real Roots*

$-\gamma_e$ deg	l_v	n_v	λ_1	v_1a_{1v}	p_1a_{1v}	r_1a_{1v}	φ_1a_{1v}	ψ_1a_{1v}	λ_2	v_2a_{2v}	p_2a_{2v}	r_2a_{2v}	φ_2a_{2v}	ψ_2a_{2v}
0	0	0·024	0·0130	0·0014	0·0018	0·0126	0·1381	0·9704	−3·4820	0·0019	0·1010	0·0036	−0·0290	−0·0010
30			−0·0361	−0·0033	−0·0045	−0·0357	0·1235	0·9875	−3·4865	0·0014	0·0876	0·0027	−0·0251	−0·0008
60			−0·0773	−0·0057	−0·0056	−0·0772	0·0730	0·9992	−3·4955	0·0005	0·0504	0·0009	−0·0144	−0·0003
90			−0·0931	−0·0061	0	−0·0934	0	1·0028	3·5	0	0	0	0	0
0	0	0·096	0·0132	0·0009	0·0018	0·0129	0·1397	0·9814	−3·4934	0·0032	0·2659	0·0035	−0·0761	−0·0010
30			−0·0363	−0·0022	−0·0045	−0·0360	0·1239	0·9900	−3·4950	0·0024	0·2322	0·0027	−0·0664	−0·0008
60			−0·0774	−0·0043	−0·0056	−0·0772	0·0729	0·9974	−3·4983	0·0008	0·1348	0·0009	−0·0385	−0·0003
90			−0·0932	−0·0050	0	−0·0932	0	1·0062	−3·5	0	0	0	0	0
0	−0·12	0·024	−0·0256	−0·0016	0·0062	−0·0222	−0·2401	0·8673	−3·8110	0·0668	4·0693	0·1411	−1·0678	−0·0370
30			−0·0656	−0·0036	0·0138	−0·0579	−0·2101	0·8832	−3·7744	0·0598	4·1588	0·1258	−1·1018	−0·0333
60			−0·0931	−0·0049	0·0224	−0·0860	−0·2411	0·9242	−3·6691	0·0383	4·4132	0·0781	−1·2028	−0·0213
90			−0·0931	−0·0061	0·0357	−0·0934	−0·3832	1·0028	−3·5	0	4·8749	0	−1·3928	0
0	−0·12	0·096	−0·0175	−0·0010	0·0032	−0·0167	−0·1798	0·9515	−3·7201	0·0330	2·9008	0·0431	−0·7798	−0·0115
30			−0·0617	−0·0032	0·0112	−0·0593	−0·1816	0·9613	−3·6927	0·0209	2·9128	0·0373	−0·7888	−0·0101
60			−0·0918	−0·0047	0·0209	−0·0899	−0·2273	0·9788	−3·6151	0·0170	2·9062	0·0207	−0·8039	−0·0057
90			−0·0932	−0·0050	0·0294	−0·0932	−0·3157	1·0002	−3·5	0	2·8720	0	−0·8206	0

TABLE 3—*continued*

(ii) *Complex Roots.—Period*

$-\gamma_e$ deg	l_v	n_v	$\frac{6\cdot28}{s}\hat{t}$	$\frac{0\cdot110s}{r}$	$2\lvert v_3\alpha_{3v}\rvert$	$2\lvert p_3\alpha_{3v}\rvert$	$2\lvert r_3\alpha_{3v}\rvert$	$2\lvert \varphi_3\alpha_{3v}\rvert$	$2\lvert \psi_3\alpha_{3v}\rvert$
0	0	0·024	5·0657	0·073	0·9972	0·2238	1·6310	0·1349	0·9719
30			5·0831	0·813	1·0020	0·1940	1·6399	0·1175	0·9933
60			5·0997	0·913	1·0052	0·1164	1·6453	0·0680	1·0017
90			5·1070	0·962	1·0065	0	1·6461	0	1·0045
0	0	0·096	2·5439	0·814	0·9989	0·3648	3·2652	0·1106	0·9900
30			2·5483	0·862	1·0021	0·3163	3·2762	0·0962	0·9960
60			2·5538	0·908	1·0054	0·1826	3·2857	0·0557	1·0019
90			2·5563	0·928	1·0067	0	3·2893	0	1·0043
0	—0·12	0·024	4·2451	3·322	0·9367	4·7444	1·6362	1·4211	0·8350
30			4·3352	3·342	0·9449	4·8041	1·6352	1·5036	0·8522
60			4·6097	1·947	0·9668	5·0249	1·6334	2·7815	0·9041
90			5·1070	0·962	1·0065	5·4509	1·6461	1·7769	1·0045
0	—0·12	0·096	2·4622	1·184	0·9703	4·1736	3·2040	1·2307	0·9448
30			2·4760	1·210	0·9762	4·2030	3·2185	1·2465	0·9545
60			2·5105	1·108	0·9893	4·3056	3·2485	1·2937	0·9701
90			2·5563	0·928	1·0067	4·4718	3·2893	1·3649	1·0043

All constant terms zero.

TABLE 4

Response to Constant Applied Rolling Moment

(i) *Real Roots*

$-\gamma_e$ deg	l_v	n_v	λ_1	$\frac{v_1 a_{1l}}{\lambda_1}$	$\frac{p_1 a_{1l}}{\lambda_1}$	$\frac{r_1 a_{1l}}{\lambda_1}$	$\frac{\phi_1 a_{1l}}{\lambda_1}$	$\frac{\psi_1 a_{1l}}{\lambda_1}$	λ_2	$\frac{v_2 a_{2l}}{\lambda_2}$	$\frac{p_2 a_{2l}}{\lambda_2}$	$\frac{r_2 a_{2l}}{\lambda_2}$	$\frac{\phi_2 a_{2l}}{\lambda_2}$	$\frac{\psi_2 a_{2l}}{\lambda_2}$
0	0	0·024	0·0130	0·2257	0·2824	1·9841	21·6764	152·3000	—3·4820	—0·0055	—0·2877	—0·0103	0·0826	0·003
30			—0·0361	—0·0600	—0·0806	—0·6431	2·2308	17·7923	—3·4865	—0·0047	—0·2872	—0·0090	0·0824	0·0026
60			—0·0773	—0·0131	—0·0122	—0·1909	0·1583	2·3122	—3·4935	—0·0027	—0·2862	—0·0052	0·0819	0·0015
90			—0·0931	0	0	0	0	0	—3·5	0	—0·2857	0	0·0816	0
0	0	0·096	0·0132	0·0379	0·2831	1·9894	21·5186	151·1966	—3·4934	—0·0037	—0·2851	—0·0037	0·0816	0·0011
30			—0·0363	—0·0389	—0·0802	—0·6394	2·2067	17·5993	—3·4950	—0·0030	—0·2852	—0·0033	0·0816	0·0009
60			—0·0774	—0·0099	—0·0121	—0·1771	0·1566	2·2874	—3·4983	—0·0017	—0·2856	—0·0019	0·0035	0·0006
90			—0·0932	0	0	0	0	0	—3·5	0	—0·2857	0	0·0816	0
0	—0·12	0·024	—0·0256	—0·0492	0·1865	—0·6736	—7·2771	26·2881	—3·8110	—0·0038	—0·2287	—0·0079	0·0600	0·0021
30			—0·0656	—0·0152	0·0578	—0·2433	—0·8811	3·7087	—3·7744	—0·0034	—0·2344	—0·0071	0·0621	0·0019
60			—0·0931	—0·0066	0·0309	—0·1165	—0·3321	1·2512	—3·6691	—0·0022	—0·2522	—0·0045	0·0687	0·0012
90			—0·0931	0	0	0	0	0	—3·5	0	—0·2857	0	0·0816	0
0	—0·12	0·096	—0·0175	—0·0777	0·2535	—1·3416	—14·4615	76·5296	—3·7201	—0·0029	—0·2515	—0·0037	0·0676	0·0010
30			—0·0617	—0·0193	0·0644	—0·3414	—1·0434	5·5295	—3·6927	—0·0021	—0·2555	—0·0033	0·0692	0·0009
60			—0·0918	—0·0073	0·0334	—0·1408	—0·3633	1·5340	—3·6151	—0·0016	—0·2439	—0·0017	0·0675	0·0005
90			—0·0932	0	0	0	0	0	—3·5	0	—0·2857	0	0·0816	0

TABLE 4—*continued*

(ii) *Complex Roots*

$-\gamma_e$ deg	l_v	n_v	Period (true sec)	$\frac{0 \cdot 110s}{r}$	$\frac{2\|v_3 a_{3l}\|}{\sqrt{(r^2+s^2)}}$	$\frac{2\|p_3 a_{3l}\|}{\sqrt{(r^2+s^2)}}$	$\frac{2\|r_3 a_{3l}\|}{\sqrt{(r^2+s^2)}}$	$\frac{2\|\phi_3 a_{3l}\|}{\sqrt{(r^2+s^2)}}$	$\frac{2\|\psi_3 a_{3l}\|}{\sqrt{(r^2+s^2)}}$	Q_ϕ	Q_ψ
0	0	0·024	5·0657	0·728	0·0261	0·0059	0·0555	0·0035	0·0555	0	—2·0
30			5·0821	0·813	0·0228	0·0058	0·0488	0·0027	0·0373	0·3639	0·6305
60			5·0997	0·913	0·0132	0·0014	0·0216	0·0009	0·0132	0·2972	0·1721
90			5·1070	0·962	0	0	0	0	0	0·2857	0
0	0	0·096	2·5439	0·814	0·0054	0·0019	0·0175	0·0006	0·0053	0	—2·0
30			2·5483	0·862	0·0047	0·0015	0·0152	0·0004	0·0046	0·3639	0·6305
60			2·5538	0·908	0·0027	0·0004	0·0088	0	0·0026	0·2972	0·1721
90			2·5563	0·928	0	0	0	0	0	0	0
0	—0·12	0·024	4·2451	3·322	0·0161	0·0813	0·0280	0·0415	0·0143	0	0·6667
30			4·3352	3·312	0·0147	0·0747	0·0254	0·0389	0·0133	0·1371	0·2375
60			4·6097	1·947	0·0100	0·0520	0·0169	0·0288	0·0094	0·1942	0·1124
90			5·1070	0·962	0	0	0	0	0	0·2857	0
0	—0·12	0·096	2·4622	1·184	0·0047	0·0203	0·0156	0·0060	0·0046	0	1·3333
30			2·4760	1·210	0·0035	0·0179	0·0137	0·0053	0·0041	0·1929	0·3342
60			2·5105	1·108	0·0025	0·0110	0·0083	0·0033	0·0025	0·2356	0·1364
90			2·5563	0·928	0	0	0	0	0	0	0

Linear terms in $\hat{p}$, $\hat{v}$, $\hat{r}$ zero.

TABLE 5—*continued*

(ii) *Complex Roots*

$-\gamma_e$ deg	l_v	n_v	Period (true sec)	$\frac{0\cdot110s}{r}$	$\frac{2\lvert v_3 a_{3n}\rvert}{\sqrt{(r^2+s^2)}}$	$\frac{2\lvert p_3 a_{3n}\rvert}{\sqrt{(r^2+s^2)}}$	$\frac{2\lvert r_3 a_{3n}\rvert}{\sqrt{(r^2+s^2)}}$	$\frac{2\lvert \phi_3 a_{3n}\rvert}{\sqrt{(r^2+s^2)}}$	$\frac{2\lvert \psi_3 a_{3n}\rvert}{\sqrt{(r^2+s^2)}}$	$Q\phi$	$Q\psi$
0	0	0·024	5·0657	0·728	0·3699	0·0830	0·6046	0·0500	0·3642	0	0
30			5·0821	0·813	0·3724	0·0721	0·6094	0·0437	0·3691	0	0
60			5·0997	0·913	0·3742	0·0416	0·6124	0·0253	0·3729	0	0
90			5·1070	0·962	0·3748	0	0·6133	0	0·3742	0	0
0	0	0·096	2·5439	0·814	0·0931	0·0340	0·3042	0·3103	0·0922	0	0
30			2·5488	0·862	0·0939	0·0295	0·3053	0·0090	0·0928	0	0
60			2·5538	0·908	0·0937	0·0170	0·3063	0·0052	0·0934	0	0
90			2·5543	0·928	0·0939	0	0·3067	0	0·0936	0	0
0	−0·12	0·024	4·2451	3·322	0·2446	1·2389	0·4273	0·6322	0·2180	0	5·0
30			4·3852	3·342	0·2566	1·3047	0·4441	0·6800	0·2314	1·0201	1·7809
60			4·6097	1·947	0·2956	1·5305	0·4994	0·8505	0·2765	1·4566	0·8432
90			5·1070	0·962	0·3748	2·0308	0·6133	1·2393	0·3742	2·1029	0
0	−0·12	0·096	2·4622	1·184	0·0848	0·3646	0·2799	0·1075	0·0825	0	2·5
30			2·4760	1·210	0·0860	0·3703	0·2835	0·1098	0·0841	0·3617	0·6266
60			2·5105	1·108	0·0892	0·3884	0·2930	0·1167	0·0880	0·4417	0·2557
90			2·5563	0·928	0·0939	0·4170	0·3067	0·1273	0·0936	0·5357	0

Linear terms in $\hat{p}$, $\hat{v}$, $\hat{r}$ all zero.

TABLE 6

Response to Initial Angle of Yaw

(i) *Real Roots*

$-\gamma_e$ deg	l_v	n_v	λ_1	$v_1 a_{1\psi}$	$p_1 a_{1\psi}$	$r_1 a_{1\psi}$	$\phi_1 a_{1\psi}$	$\psi_1 a_{1\psi}$	λ_2	$v_2 a_{2\psi}$	$p_2 a_{2\psi}$	$r_2 a_{2\psi}$	$\phi_2 a_{2\psi}$	$\psi_2 a_{2\psi}$
0	0	0·024	0·0130	0	0	0	0	0	−3·4820	0	0	0	0	0
30			−0·0361	−0·0043	−0·0058	−0·0463	0·1602	1·2808	−3·4865	0	0·0012	0	−0·0003	0
60			−0·0773	−0·0059	−0·0059	−0·0817	0·0767	1·0498	−3·4955	0	0·0012	0	−0·0003	0
90			−0·0931	−0·0061	0	−0·0940	0	1·0098	−3·5	0	0	0	0	0
0	0	0·096	0·0132	0	0	0	0	0	−3·4934	0	0	0	0	0
30			−0·0363	−0·0028	−0·0058	−0·0464	0·1598	1·2773	−3·4950	0	0·0031	0	−0·0009	0
60			−0·0774	−0·0045	−0·0059	−0·0810	0·0764	1·0456	−3·4983	0	0·0031	0	−0·0009	0
90			−0·0932	−0·0061	0	−0·0940	0	1·0098	−3·5	0	0	0	0	0
0	−0·12	0·024	−0·0256	0	0	0	0	0	−3·8110	0	0	0	0	0
30			−0·0656	−0·0026	0·0098	−0·0414	−0·1501	0·6309	−3·7744	0·0007	0·0516	0·0016	−0·0137	−0·0004
60			−0·0931	−0·0043	0·0196	−0·0750	−0·2102	0·8060	−3·6691	0·0008	0·0977	0·0017	−0·0266	−0·0005
90			−0·0931	−0·0061	0·0359	−0·0940	−0·3858	1·0098	−3·5	0	0·1306	0	−0·0373	0
0	−0·12	0·096	−0·0175	0	0	0	0	0	−3·7201	0	0	0	0	0
30			−0·0617	−0·0024	0·0085	−0·0451	−0·1379	0·7299	−3·6927	0·0004	0·0370	0·0005	−0·0100	−0·0001
60			−0·0918	−0·0041	0·0185	−0·0795	−0·2011	0·8657	−3·6151	0·0004	0·0653	0·0005	−0·0181	−0·0001
90			−0·0932	−0·0050	0·0296	−0·0938	−0·3175	1·0059	−3·5	0	0·0769	0	−0·0220	0

TABLE 6—*continued*

(ii) *Complex Roots*

$-\gamma_e$ deg	l_v	n_v	Period (true sec)	$\frac{0\cdot110s}{r}$	$2\lvert v_3\alpha_{3\psi}\rvert$	$2\lvert p_3\alpha_{3\psi}\rvert$	$2\lvert r_3\alpha_{3\psi}\rvert$	$2\lvert \phi_3\alpha_{3\psi}\rvert$	$2\lvert \psi_3\alpha_{3\psi}\rvert$	Q_ϕ	Q_ψ
0	0	0·024	5·0657	0·728	0	0	0	0	0	0	0
30			5·0821	0·813	0·0284	0·0055	0·0466	0·0033	0·0284	—0·1577	—1·2738
60			5·0997	0·913	0·0497	0·0056	0·0813	0·0011	0·0495	—0·0743	—1·0402
90			5·1070	0·962	0·0576	0	0·0942	0	0·0204	0	—1·0
0	0	0·096	2·5499	0·813	0	0	0	0	0	0	0
30			2·5483	0·862	0·0143	0·0045	0·0467	0·0014	0·0142	—0·1577	—1·2738
60			2·5538	0·908	0·0249	0·0045	0·0813	0·0014	0·0248	—0·0743	—1·0402
90			2·5563	0·928	0·0288	0	0·0941	0	0·0287	0	—1·0
0	—0·12	0·024	4·2451	3·322	0	0	0	0	0	0	0
30			4·3352	3·342	0·0231	0·1173	0·0399	0·0617	0·0208	0·2148	—0·6283
60			4·6097	1·947	0·0435	0·2258	0·0734	0·1250	0·0406	0·3399	—0·8011
90			5·1070	0·962	0·0576	0·3118	0·0942	0·1903	0·0675	0·5714	—1·0
0	—0·12	0·096	2·4622	1·184	0	0	0	0	0	0	0
30			2·4760	1·210	0·0136	0·0584	0·0447	0·0173	0·0133	0·1515	—0·7274
60			2·5105	1·108	0·0241	0·1050	0·0792	0·0316	0·0238	0·2356	—0·8613
90			2·5563	0·928	0·0288	0·1280	0·0941	0·0396	0·0287	0·3511	—1·0

Constant terms in $\hat{p}$, $\hat{v}$, $\hat{r}$ all zero.

(92909)

TABLE 7

Response to Initial Angle of Bank

(i) *Real Roots*

$-\gamma_e$ deg	l_v	n_v	λ_1	$v_1a_{1\phi}$	$p_1a_{1\phi}$	$r_1a_{1\phi}$	$\phi_1a_{1\phi}$	$\psi_1a_{1\phi}$	λ_2	$v_2a_{2\phi}$	$p_2a_{2\phi}$	$r_2a_{2\phi}$	$\phi_2a_{2\phi}$	$\psi_2a_{2\phi}$
0	0	0·024	0·0130	0·0104	0·0129	0·0910	0·9939	6·9830	−3·4820	−0·0001	−0·0027	−0·0001	0·0008	0
30			−0·0361	0·0075	0·0100	0·0802	−0·2776	−2·2187	−3·4865	0	−0·0020	−0·0001	0·0006	0
60			−0·0773	0·0034	0·0034	0·0470	−0·0444	−0·6077	−3·4955	0	−0·0007	0	0·0002	0
90			−0·0931	0	0	0	0	0	−3·5	0	0	0	0	0
0	0	0·096	0·0132	0·0061	0·0131	0·0920	0·9952	6·9923	−3·4934	−0·0001	−0·0071	−0·0001	0·0020	0
30			−0·0363	0·0049	0·0101	0·0804	−0·2768	−2·2125	−3·4950	−0·0001	−0·0054	−0·0001	0·0015	0
60			−0·0074	0·0026	0·0034	0·0469	−0·0442	−0·6053	−3·4983	0	−0·0018	0	0·0005	0
90			0·0932	0	0	0	0	0	−3·5	0	0	0	0	0
0	−0·12	0·024	−0·0256	0·0059	−0·0225	0·0813	0·8784	−3·1731	−3·8110	−0·0016	−0·1001	−0·0035	0·0263	0·0009
30			−0·0656	0·0045	−0·0171	0·0717	0·2600	−1·0929	−3·7744	−0·0013	−0·0895	−0·0027	0·0237	0·0007
60			−0·0931	0·0025	−0·0113	0·0434	0·1217	−0·4666	−3·6691	−0·0005	−0·0565	−0·0010	0·0154	0·0003
90			−0·0931	0	0	0	0	0	−3·5	0	0	0	0	0
0	−0·12	0·096	−0·0175	0·0052	−0·0169	0·0892	0·9616	−5·0887	−3·7201	−0·0008	−0·0731	−0·0011	0·0197	0·0003
30			−0·0617	0·0042	−0·0148	0·0781	0·2389	−1·2643	−3·6927	−0·0006	−0·0641	−0·0008	0·0173	0·0002
60			−0·0918	0·0024	−0·0107	0·0460	0·1164	−0·5011	−3·6151	−0·0002	−0·0378	−0·0003	0·0105	0·0001
90			−0·0932	0	0	0	0	0	−3·5	0	0	0	0	0

B*

TABLE 7—*continued*

(ii) *Complex Roots*

$-\gamma_e$ deg	l_v	n_v	Period (true sec)	$\frac{0\cdot110s}{r}$	$2\lvert v_3\alpha_{3\phi}\rvert$	$2\lvert p_3\alpha_{3\phi}\rvert$	$2\lvert r_3\alpha_{3\phi}\rvert$	$2\lvert \phi_3\alpha_{3\phi}\rvert$	$2\lvert \psi_3\alpha_{3\phi}\rvert$	Q_ϕ	Q_ψ
0	0	0·024	5·0657	0·728	0·0563	0·0126	0·0921	0·0076	0·0555	−1·0	−7·0
30			5·0821	0·813	0·0493	0·0095	0·0807	0·0058	0·0489	0·2732	2·2066
60			5·0997	0·913	0·0289	0·0032	0·0471	0·0019	0·0287	0·0430	0·6022
90			5·1070	0·962	0	0	0	0	0	0	0
0	0	0·096	2·5439	0·814	0·0284	0·0104	0·0928	0·0031	0·0281	−1·0	−7·0
30			2·5483	0·862	0·0247	0·0078	0·0809	0·0024	0·0246	0·2732	2·2066
60			2·5538	0·908	0·0144	0·0026	0·0471	0·0008	0·0081	0·0430	0·6022
90			2·5563	0·928	0	0	0	0	0	0	0
0	−0·12	0·024	4·2451	3·322	0·0448	0·2270	0·0783	0·1154	0·0399	−1·0	3·1667
30			4·3352	3·342	0·0400	0·2033	0·0692	0·1059	0·0361	0·3720	1·0884
60			4·6097	1·947	0·0252	0·1307	0·0425	0·0724	0·0235	−0·1968	0·4638
90			5·1070	0·962	0	0	0	0	0	0	0
0	−0·12	0·096	2·4622	1·184	0·0268	0·1154	0·0886	0·0240	0·0261	−1·0	5·0833
30			2·4760	1·210	0·0235	0·1012	0·0775	0·0300	0·0230	−0·2729	1·2601
60			2·5105	1·108	0·0140	0·0608	0·0459	0·0183	0·0138	−0·1364	0·4986
90			2·5563	0·928	0	0	0	0	0	0	0

Constant terms in $\hat{p}$, $\hat{v}$, $\hat{r}$ all zero.

TABLE 8

Phase Angles for All Disturbances

$-\gamma_0$ deg	l_v	n_v	β_v	β_ϕ	β_ψ	β_l	β_n	γ_v	γ_p	γ_r	γ_ϕ	γ_ψ
0	0	0·024	1·92°	100·47°	*	39·28°	188·83°	0	115·38°	88·65°	214·06°	187·27°
30			0·96°	98·67°	278·67°	37·47°	187·91°	0	114·41°	87·89°	212·14°	185·62°
60			359·63°	96·86°	276·86°	35·67°	186·96°	0	113·98°	87·71°	210·87°	184·60°
90			359·56°	*	276·10°	*	186·57°	0	*	87·18°	*	183·73°
0	0	0·096	4·44°	102·16°	*	58·50°	187·91°	0	132·76°	85·83°	230·49°	183·57°
30			3·96°	101·26°	281·26°	58·05°	187·75°	0	132·00°	85·46°	229·38°	182·72°
60			3·49°	100·42°	280·42°	57·06°	186·98°	0	131·54°	85·18°	228·46°	182·10°
90			3·29°	*	280·01°	*	186·57°	0	*	85·08°	*	181·86°
0	−0·12	0·024	3·60°	95·51°	*	31·56°	178·77°	0	207·19°	90·57°	299·10°	182·47°
30			2·69°	94·59°	274·59°	31·02°	179·26°	0	207·02°	89·69°	298·91°	181·58°
60			1·31°	94·52°	274·52°	32·24°	182·21°	0	206·72°	88·97°	299·99°	181·65°
90			359·56°	*	276·10°	*	186·57°	0	206·17°	87·18°	302·71°	183·73°
0	−0·12	0·096	3·98°	99·30°	*	53·84°	183·05°	0	221·93°	86·49°	317·25°	181·81°
30			3·58°	98·79°	278·79°	54·34°	183·20°	0	222·34°	86·03°	317·55°	181·24°
60			3·27°	98·96°	278·96°	54·38°	184·46°	0	223·89°	85·51°	319·59°	181·20°
90			3·30°	*	280·01°	*	187·35°	0	226·25°	85·07°	323·03°	181·85°

* indicates that if either β_v or γ_v, etc., is * the sum $(\beta_v + \gamma_v)$, etc., is meaningless since the excitation of the oscillatory mode is zero.

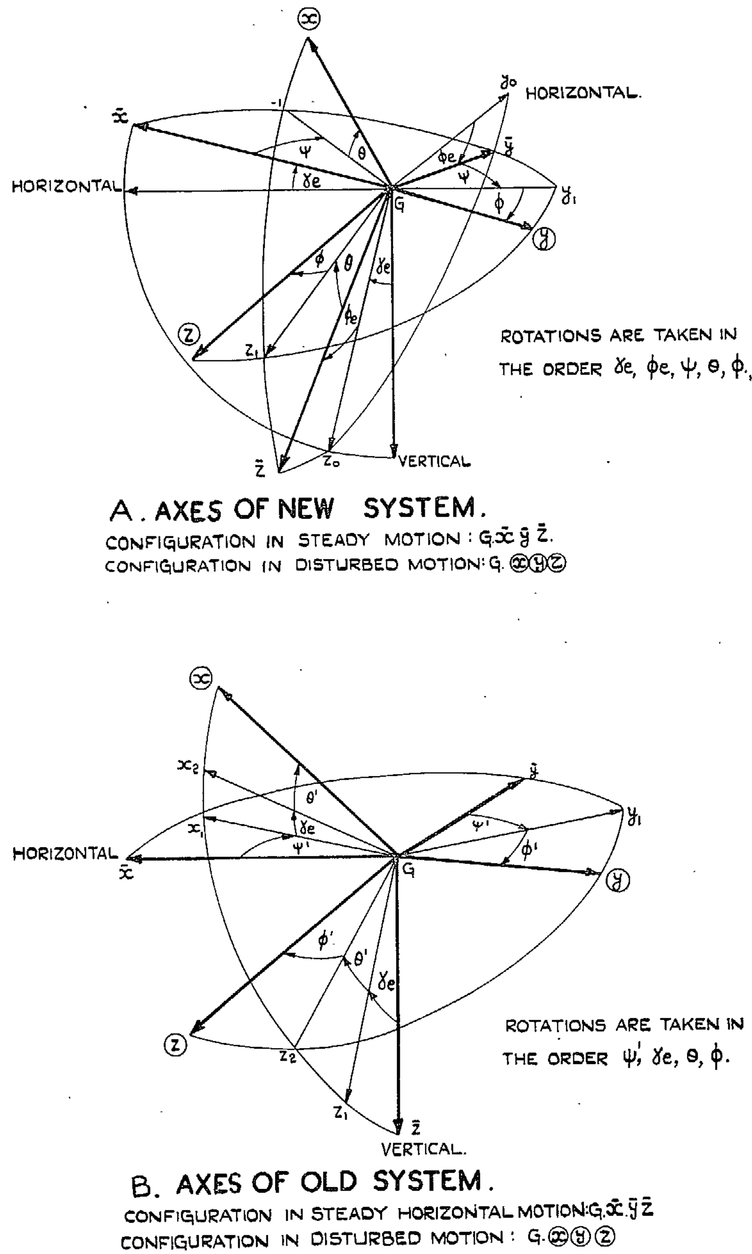

FIG. 1

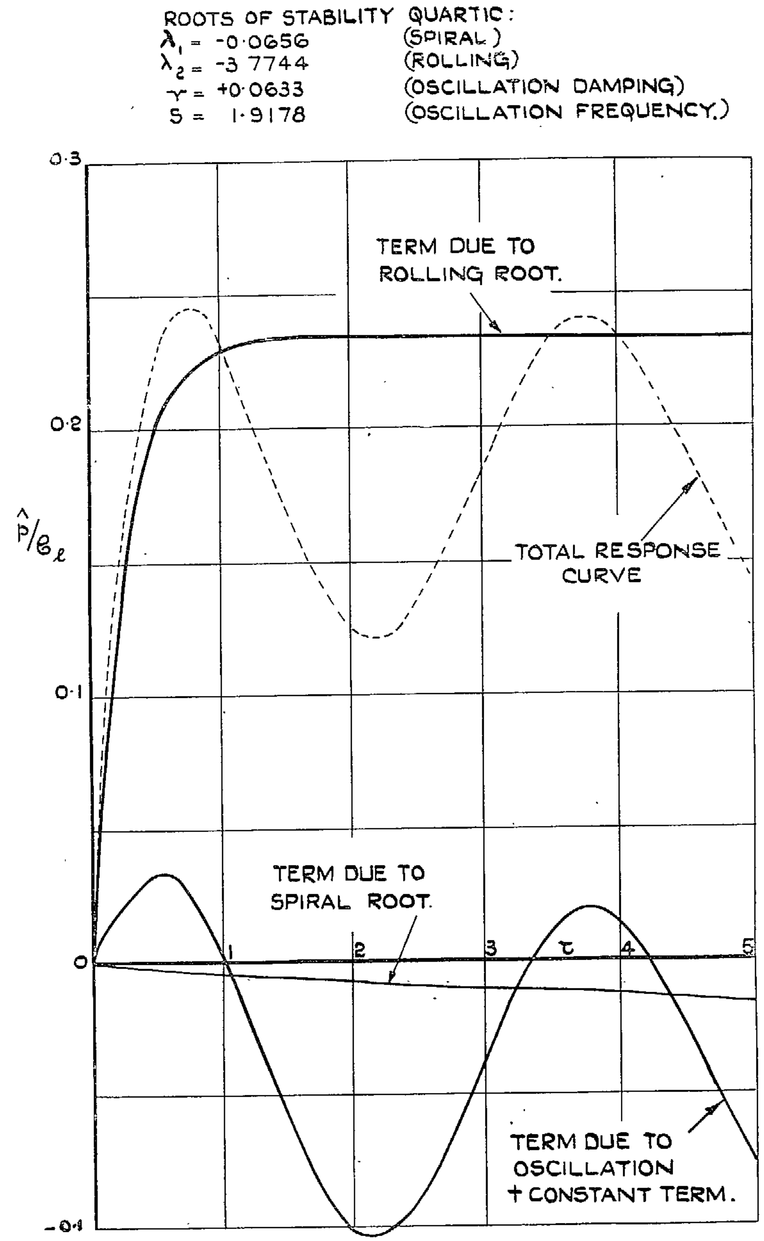

FIG. 2. Response in Rate of Roll to an Applied Rolling Moment Showing the Contributions of the Three Modes of Motion when $l = -0{\cdot}12$, $\eta_v = 0{\cdot}024$.

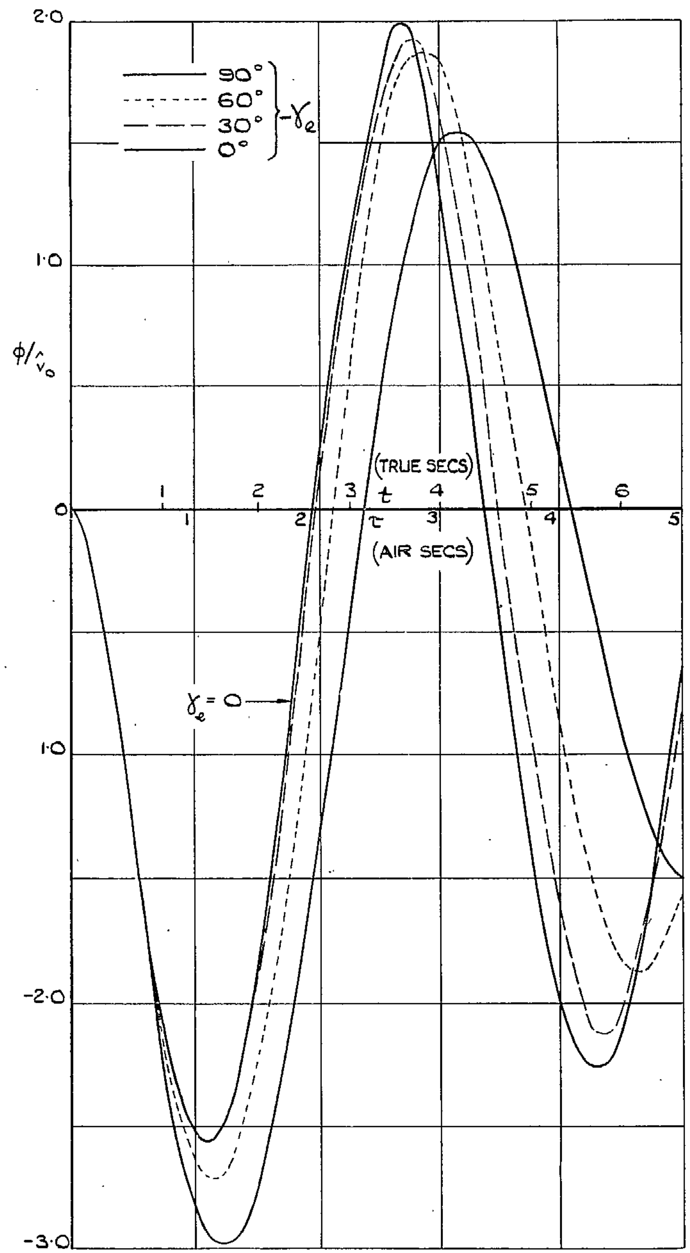

FIG. 3. Variations with α_e of the Response in Angle of Bank to a Side-gust for $n_v = 0 \cdot 024$, $l_v = -0 \cdot 12$.

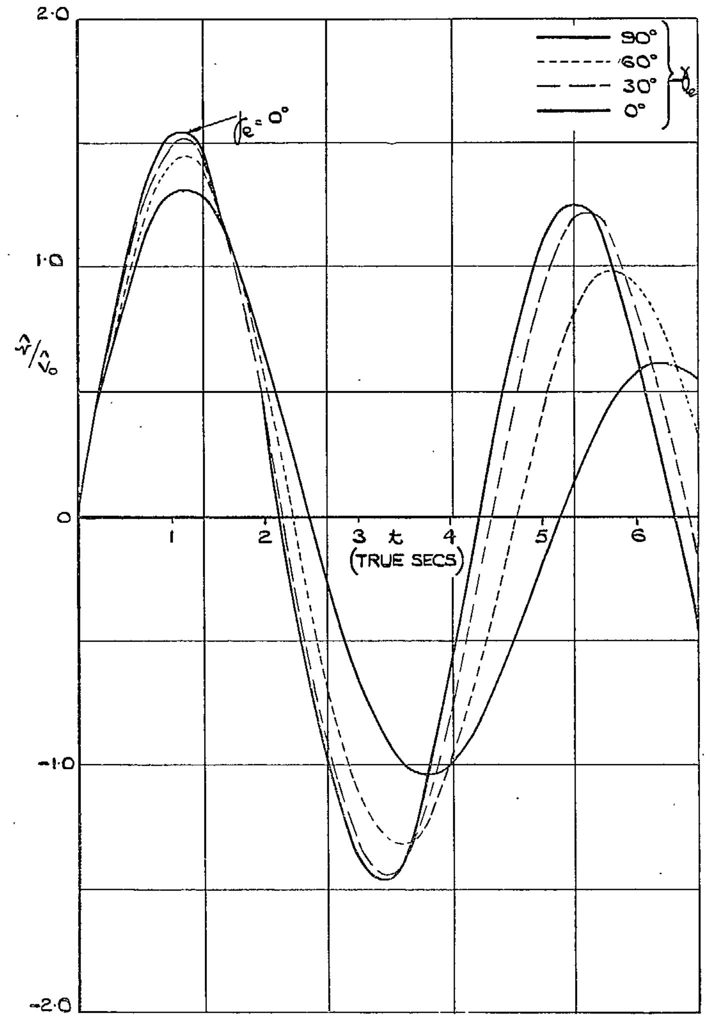

FIG. 4. Variations with α_e of the Response in Rate of Yaw to a Side-gust when $n_v = 0 \cdot 024$, $l_v = -0 \cdot 12$.

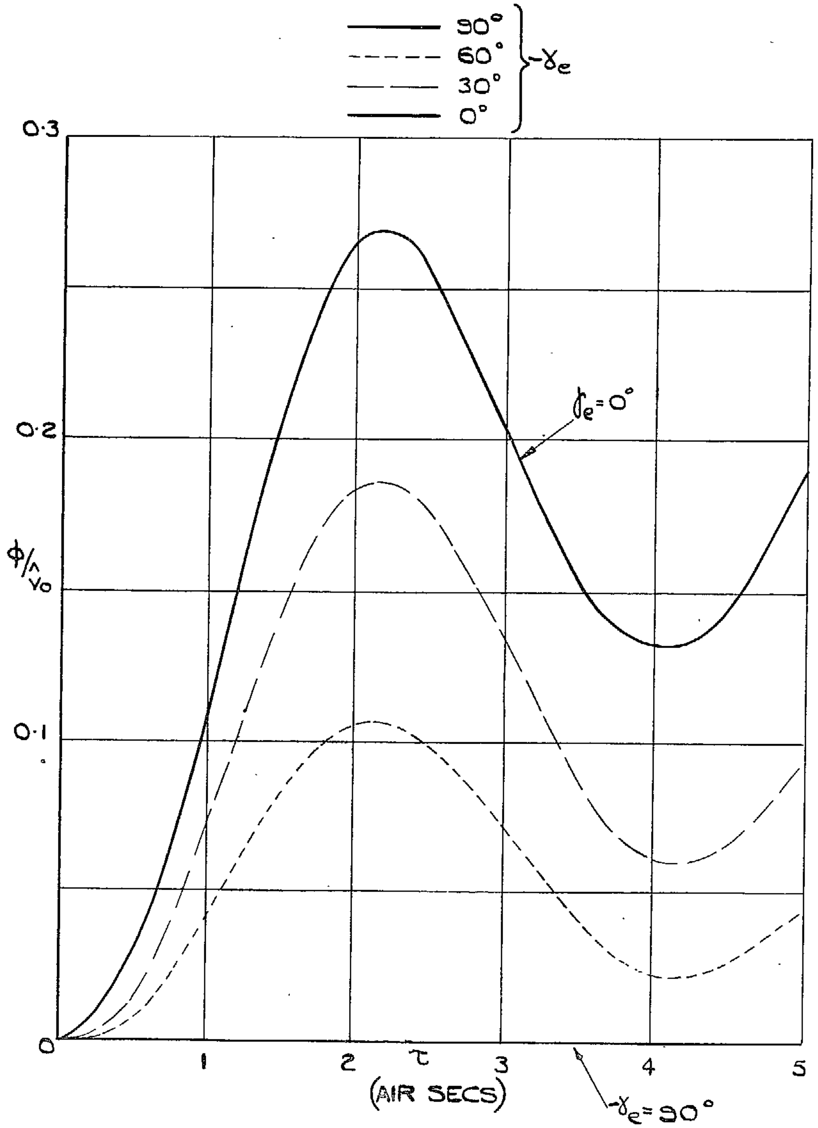

FIG. 5. Response in Angle of Bank to a Side-gust with Varying Flight-path Angle when $l_v = 0$, $n_v = 0 \cdot 024$.

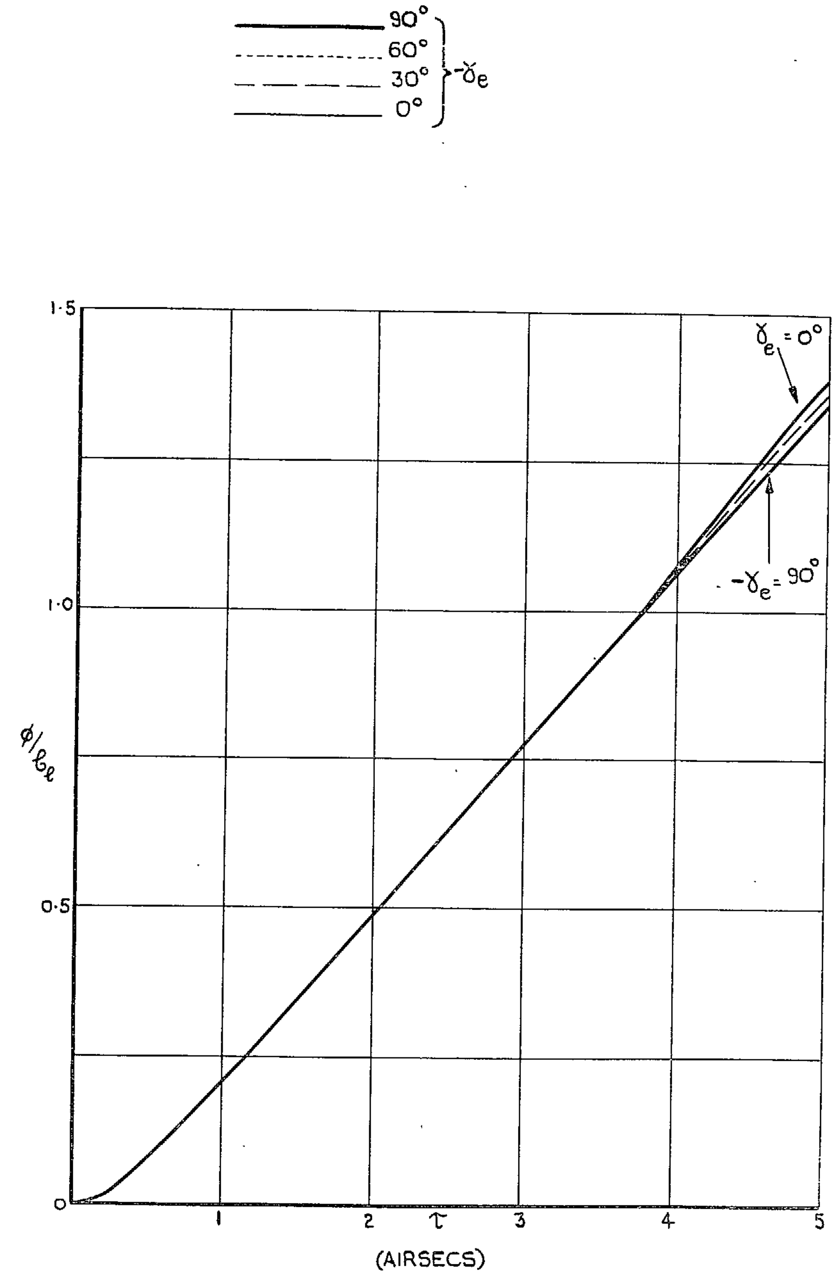

FIG. 6. Response in Angle of Bank to Applied Rolling Moment with Varying Flight-path Angle for $l_v = 0$, $n_v = 0 \cdot 024$.

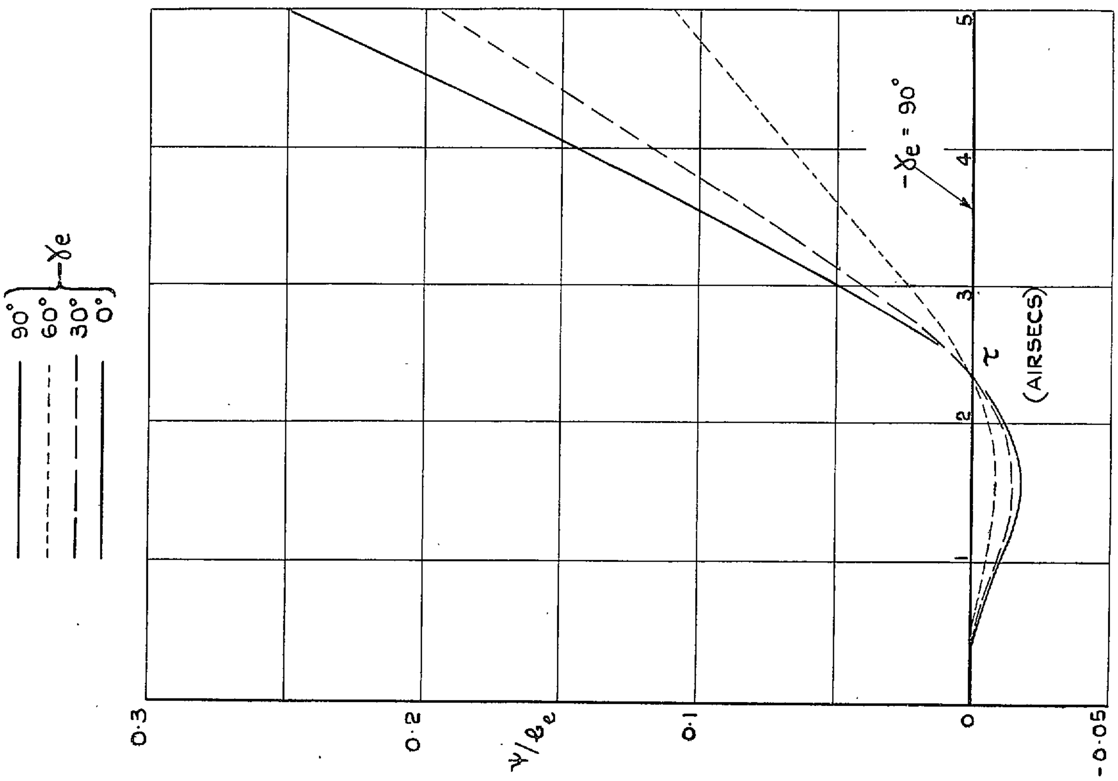

FIG. 7. Response in Angle of Yaw to an Applied Rolling Moment with Varying Flight-path Angle for $l_v = 0$, $n_v = 0 \cdot 024$.

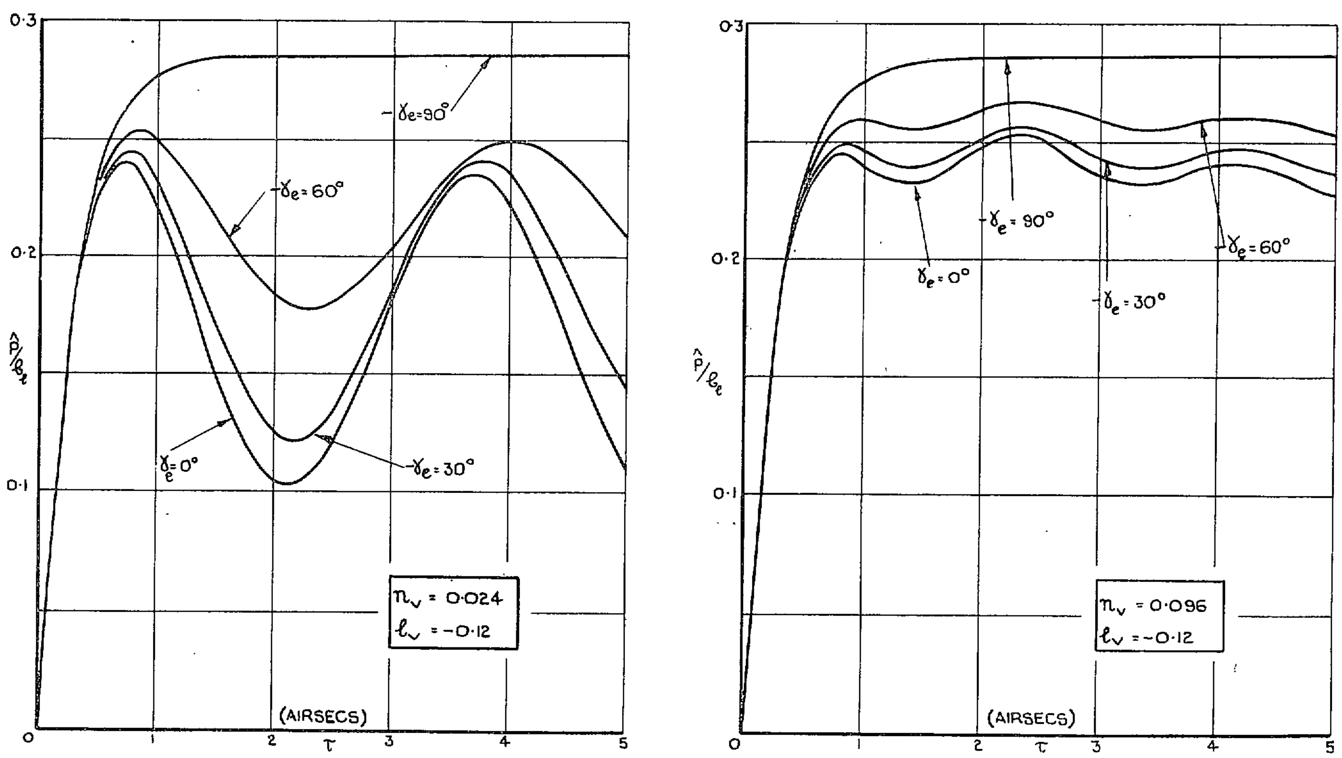

FIG. 8. Response in Rate of Roll to Applied Rolling Moment with Varying Angle of Dive.

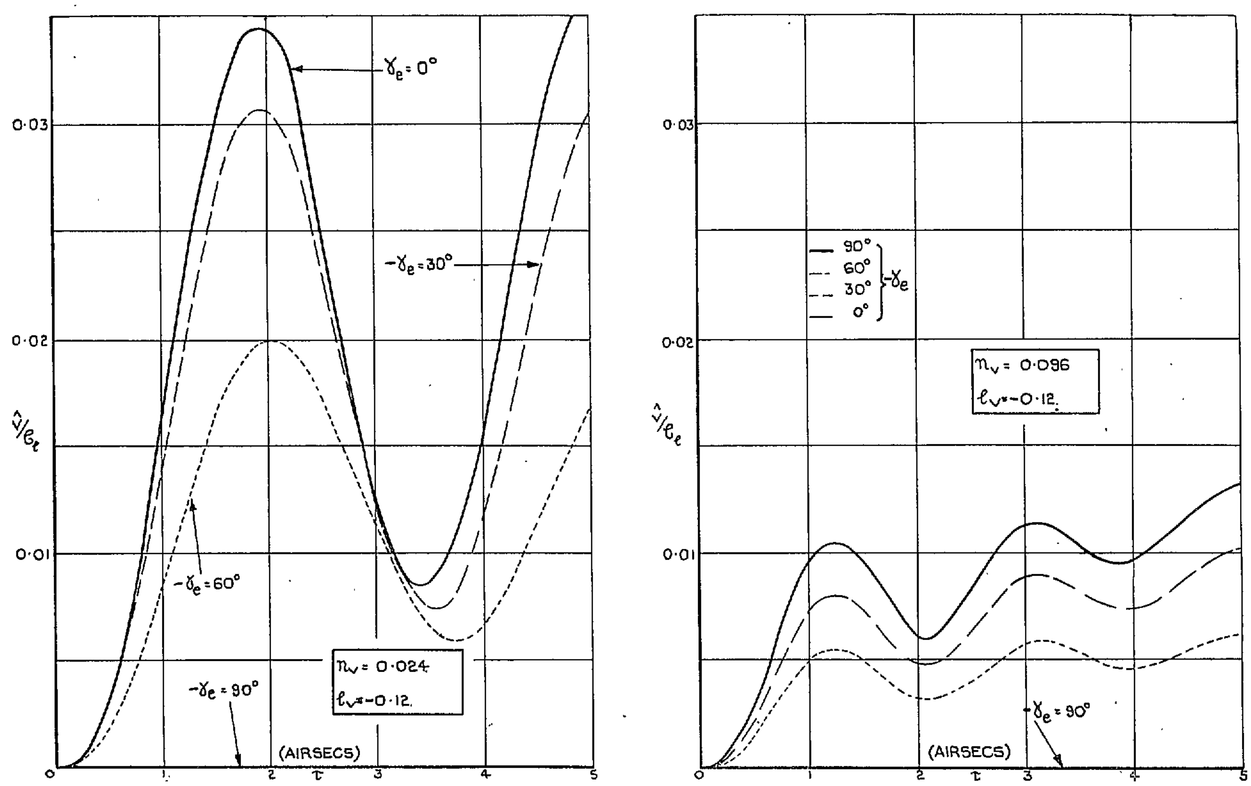

FIG. 9. Response in Angle of Sideslip to Applied Rolling Moment with Varying Angle of Dive.

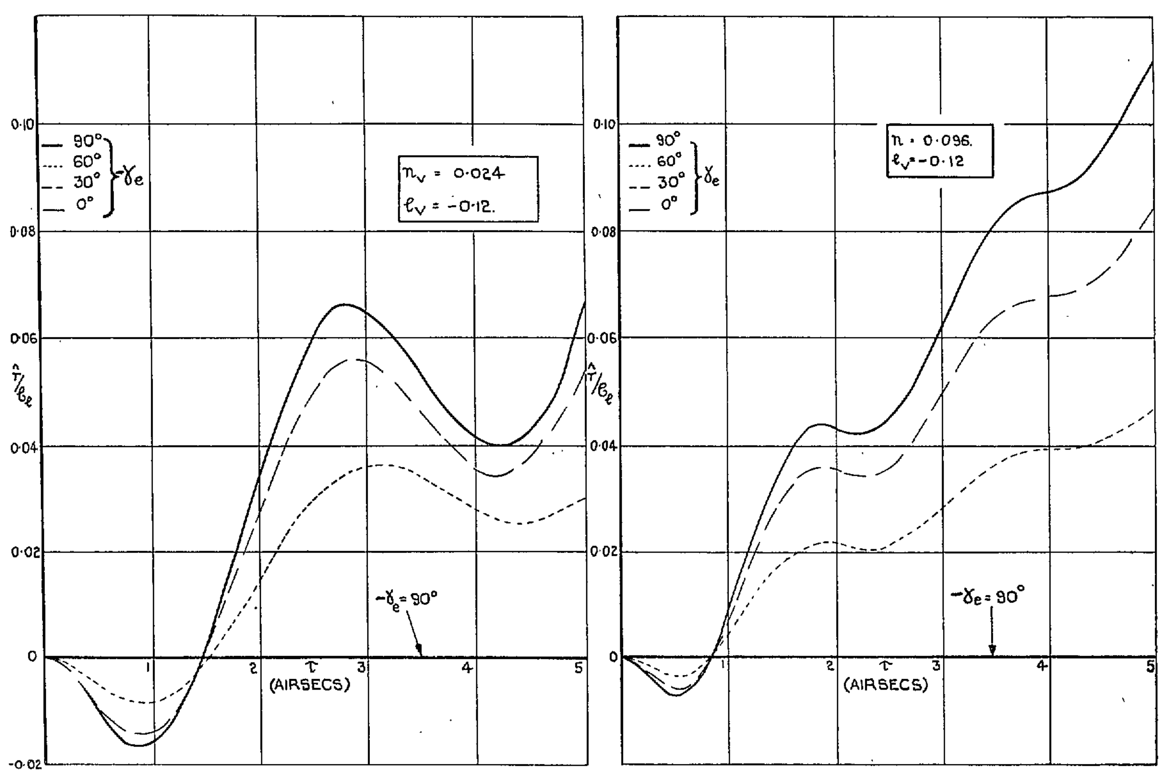

FIG. 10. Response in Rate of Yaw to Applied Rolling Moment with Varying Angle of Dive.

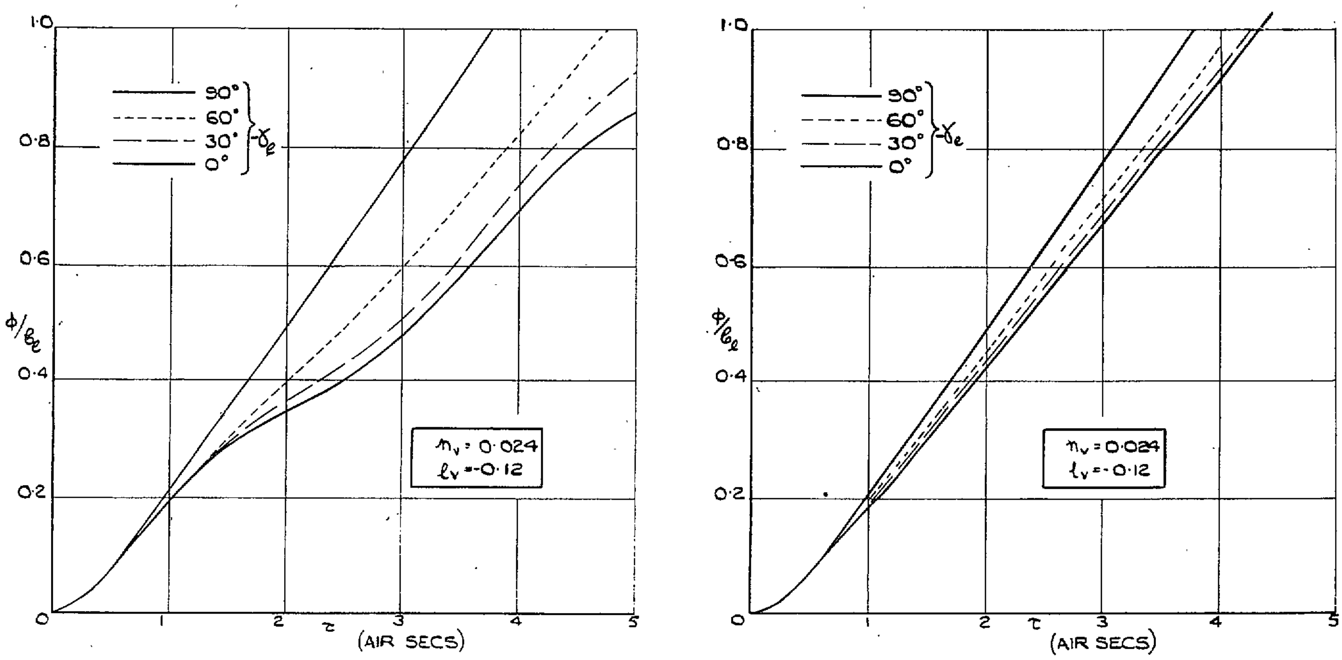

FIG. 11. Response in Angle of Bank to Applied Rolling Moment for Varying Angle of Dive.

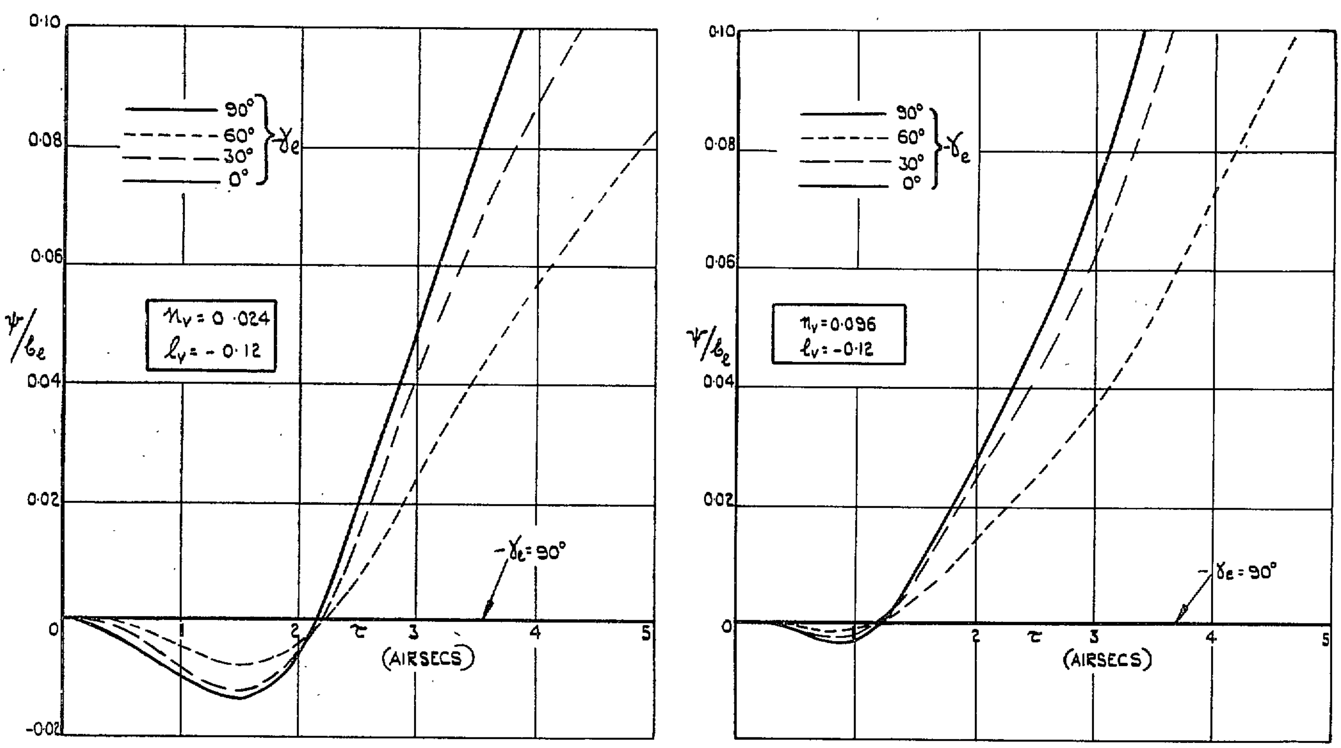

FIG. 12. Response in Angle of Yaw to Applied Rolling Moment with Varying Angle of Dive.

(92099) Wt. 13/806 K.5 12/53 Hw.

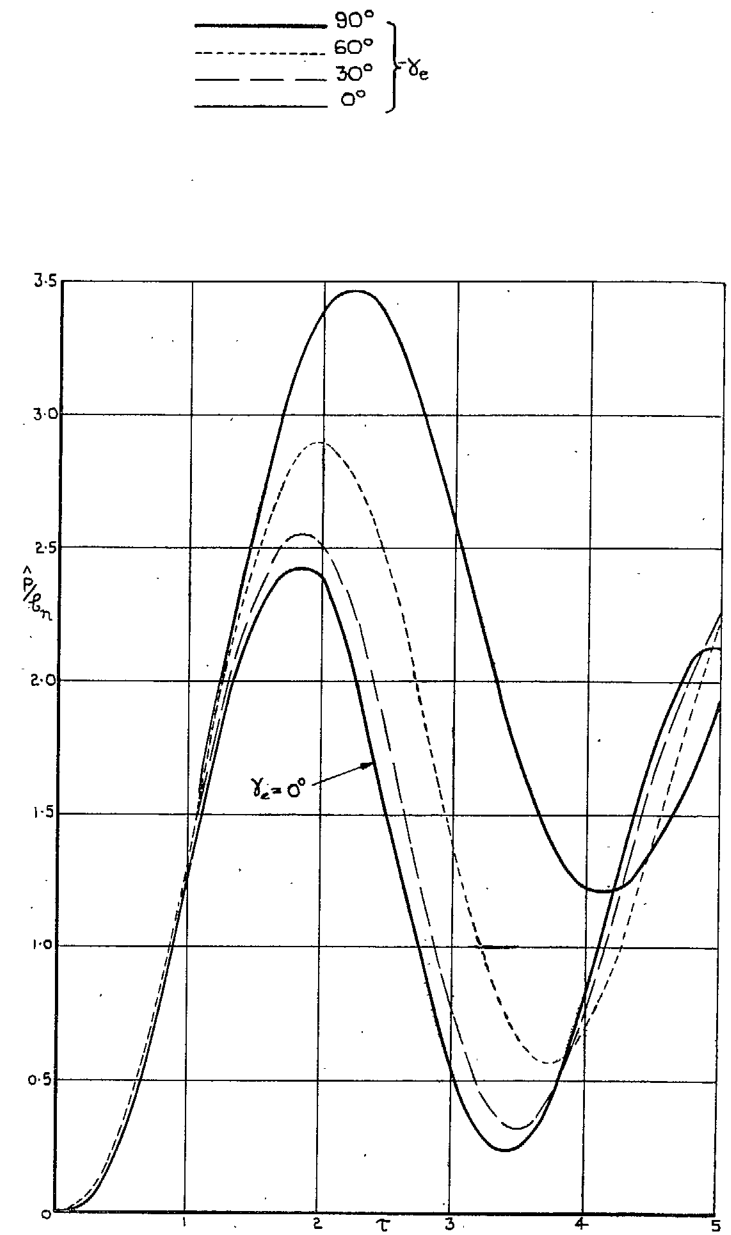

Fig. 13. Response in Rate of Roll to Applied Yawing Moment with Varying Flight-path Angle for $l_v = -0 \cdot 12$, $n_v = 0 \cdot 024$.

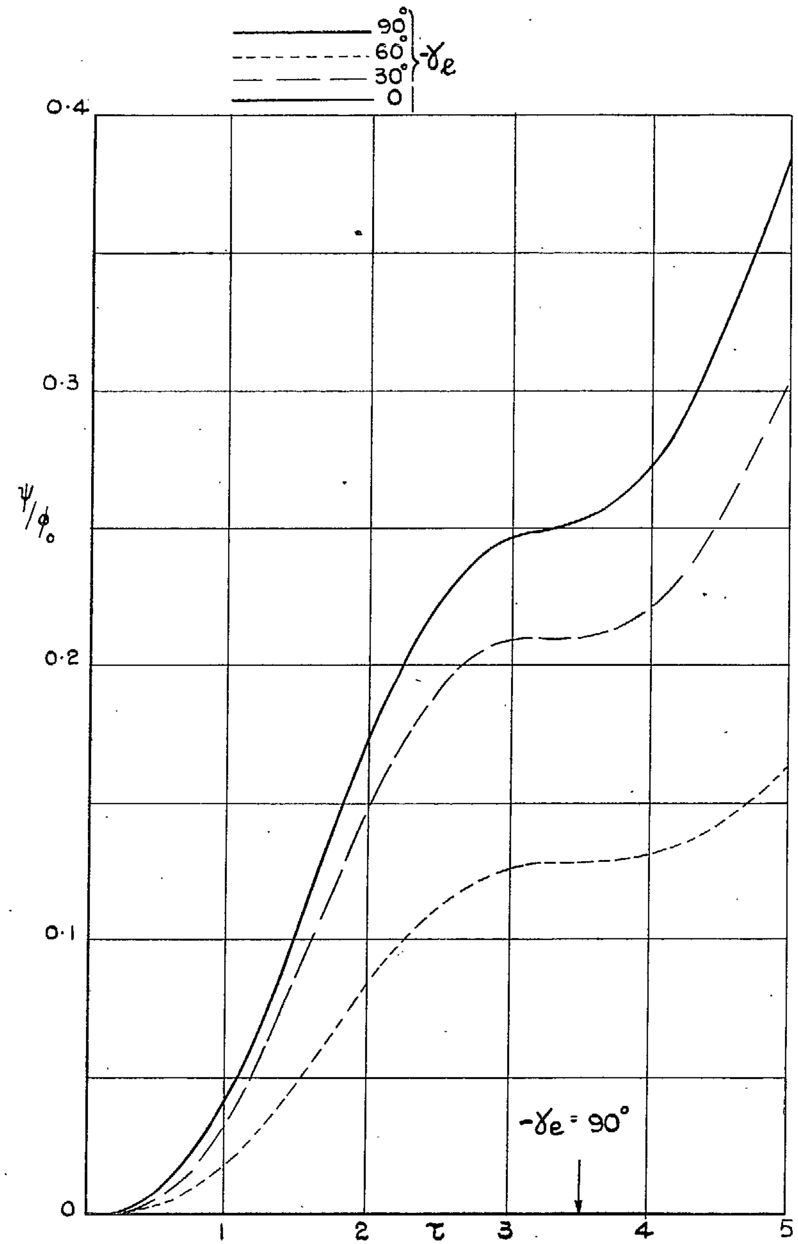

Fig. 14. Response in Angle of Yaw to Initial Angle of Bank with Varying Flight-path Angle for $l_v = -0 \cdot 12$, $n_v = 0 \cdot 024$.

PRINTED IN GREAT BRITAIN

Publications of the Aeronautical Research Council

ANNUAL TECHNICAL REPORTS OF THE AERONAUTICAL RESEARCH COUNCIL (BOUND VOLUMES)

1936 Vol. I. Aerodynamics General, Performance, Airscrews, Flutter and Spinning. 40*s.* (40*s.* 9*d.*)
Vol. II. Stability and Control, Structures, Seaplanes, Engines, etc. 50*s.* (50*s.* 10*d.*)

1937 Vol. I. Aerodynamics General, Performance, Airscrews, Flutter and Spinning. 40*s.* (40*s.* 10*d.*)
Vol. II. Stability and Control, Structures, Seaplanes, Engines, etc. 60*s.* (61*s.*)

1938 Vol. I. Aerodynamics General, Performance, Airscrews. 50*s.* (51*s.*)
Vol. II. Stability and Control, Flutter, Structures, Seaplanes, Wind Tunnels, Materials. 30*s.* (30*s.* 9*d.*)

1939 Vol. I. Aerodynamics General, Performance, Airscrews, Engines. 50*s.* (50*s.* 11*d.*)
Vol. II. Stability and Control, Flutter and Vibration, Instruments, Structures, Seaplanes, etc. 63*s.* (64*s.* 2*d.*)

1940 Aero and Hydrodynamics, Aerofoils, Airscrews, Engines, Flutter, Icing, Stability and Control, Structures, and a miscellaneous section. 50*s.* (51*s.*)

1941 Aero and Hydrodynamics, Aerofoils, Airscrews, Engines, Flutter, Stability and Control, Structures. 63*s.* (64*s.* 2*d.*)

1942 Vol. I. Aero and Hydrodynamics, Aerofoils, Airscrews, Engines. 75*s.* (76*s.* 3*d.*)
Vol. II. Noise, Parachutes, Stability and Control, Structures, Vibration, Wind Tunnels 47*s.* 6*d.* (48*s.* 5*d.*)

1943 Vol. I. (*In the press.*)
Vol. II. (*In the press.*)

ANNUAL REPORTS OF THE AERONAUTICAL RESEARCH COUNCIL—

1933–34	1*s.* 6*d.* (1*s.* 8*d.*)	1937	2*s.* (2*s.* 2*d.*)
1934–35	1*s.* 6*d.* (1*s.* 8*d.*)	1938	1*s.* 6*d.* (1*s.* 8*d.*)
April 1, 1935 to Dec. 31, 1936.	4*s.* (4*s.* 4*d.*)	1939–48	3*s.* (3*s.* 2*d.*)

INDEX TO ALL REPORTS AND MEMORANDA PUBLISHED IN THE ANNUAL TECHNICAL REPORTS, AND SEPARATELY—

April, 1950 - - - - R. & M. No. 2600. 2*s.* 6*d.* (2*s.* 7½*d.*)

AUTHOR INDEX TO ALL REPORTS AND MEMORANDA OF THE AERONAUTICAL RESEARCH COUNCIL—

1909–1949. R. & M. No. 2570. 15*s.* (15*s.* 3*d.*)

INDEXES TO THE TECHNICAL REPORTS OF THE AERONAUTICAL RESEARCH COUNCIL—

December 1, 1936 — June 30, 1939.	R. & M. No. 1850.	1*s.* 3*d.* (1*s.* 4½*d.*)
July 1, 1939 — June 30, 1945.	R. & M. No. 1950.	1*s.* (1*s.* 1½*d.*)
July 1, 1945 — June 30, 1946.	R. & M. No. 2050.	1*s.* (1*s.* 1½*d.*)
July 1, 1946 — December 31, 1946.	R. & M. No. 2150.	1*s.* 3*d.* (1*s.* 4½*d.*)
January 1, 1947 — June 30, 1947.	R. & M. No. 2250.	1*s.* 3*d.* (1*s.* 4½*d.*)
July, 1951.	R. & M. No. 2350.	1*s.* 9*d.* (1*s.* 10½*d.*)

Prices in brackets include postage.

Obtainable from

HER MAJESTY'S STATIONERY OFFICE

York House, Kingsway, London, W.C.2; 423 Oxford Street, London, W.1 (Post Orders: P.O. Box 569, London, S.E.1); 13a Castle Street, Edinburgh 2; 39, King Street, Manchester, 2; 2 Edmund Street, Birmingham 3; 1 St. Andrew's Crescent, Cardiff; Tower Lane, Bristol 1; 80 Chichester Street, Belfast, or through any bookseller

S.O. Code No. 23-2529

R. & M. No. 2529